THE ROLE OF DEFECTIVE $Na_{V1.4}$ CHANNELS IN THE MECHANISM OF HYPERKALEMIC PERIODIC PARALYSIS

By

Brooke Lucas

A thesis submitted to the Faculty of Graduate and Post-Doctoral Studies

of the University of Ottawa

in partial fulfillment of the requirements of the Degree of

Masters of Science

Department of Cellular and Molecular Medicine

Faculty of Medicine

University of Ottawa

ABSTRACT

Hyperkalemic periodic paralysis (HyperKPP) is an autosomal dominant human skeletal muscle channelopathy that causes periods of myotonic discharge and periodic paralysis due to defective $Na_{v1.4}$ sodium channels. Patients are asymptomatic at birth, attacks become short and frequent during childhood, and more severe during adolescence. Since the $Na_{v1.4}$ content in the cell membrane is relatively constant during childhood, it was hypothesized that some symptoms start with the defective $Na_{v1.4}$ channels, while other symptoms start after some changes occur in gene expression affecting other membrane channel content and/or activity. To test the hypothesis, the contractile characteristics of EDL and soleus muscles from HyperKPP mice from the age of 0.5 to 12 months were tested *in vitro.* For both EDL and soleus, contractile defects, including low force generation, instability and large unstimulated force were observed by two weeks of age. With aging, the defects did not worsen, but muscles actually showed some improvement. Considering that $Na_{v1.4}$ protein content reaches maximum at three weeks of age, the data suggests that HyperKPP symptoms are solely due to the defective $Na_{v1.4}$ channels.

TABLE OF CONTENTS

LIST OF FIGURES

LIST OF TABLES

LIST OF ABBREVIATIONS

$[\ ]_i$	intracellular concentration
$[\ ]_e$	extracellular concentration
ºC	degree Celsius
ANOVA	analysis of variance
AP	action potential
Ca^{2+}	calcium ion
Cl^-	chloride ion
ClC-1	chloride channel
DHP	dihydropyridine receptor
EDL	extensor digitorum longus
E_m	resting membrane potential
E_{rev}	equilibrium reversal potential
G_{Na}	sodium conductance
HyperKPP	Hyperkalemic periodic paralysis
HypoKPP	Hypokalemic periodic paralysis
Hz	hertz
K^+	potassium ion
K_{ATP} channel	ATP-sensitive K^+ channel
K_{ir}	inward-rectifying potassium channel
K_v	voltage-sensitive K^+ channel
L.S.D.	least significant difference
mM	millimolar

mL	milliliter
ms	millisecond
mV	millivolt
n	number of sample
Na^+	sodium ion
Na_v	voltage-sensitive sodium channel
N/cm^2	Newton per centimeter square
PAM	Potassium-aggravated myotonia
PC	Paramyotonia congenita
pS	picosiemens
S.E.	standard error
SR	sarcoplasmic reticulum
t-test	student t-test
WT	wild-type

ACKNOWLEDGEMENTS

First, I would like to thank my supervisor and mentor, Jean-Marc, for his patience, knowledge, and great sense of humour. Most of all, Jean-Marc helped keep me calm through many stressful times, and was always very reassuring when I would get “nervous.” I have learned so much from Jean-Marc, and will always be grateful for all of his support.

I would also like to thank my advisory committee, Dr. Bernard Jasmin and Dr. Michael Jonz for their excellent advice, suggestions, and guidance.

I owe many thanks to all of my lab members, both past and present. In particular, I owe a huge thank you to my best friend and lab mate, Kyle Scott. I wouldn’t have been able to do all of this without you. You have always been there for me- during stressful times, making me laugh, and even helping me change the gas tank regulators!

Last but not least, I owe a huge thank you to my wonderful parents for all of their support and assistance during my grad school experience. I truly would not have been able to do this without you.

CHAPTER ONE

INTRODUCTION

The contraction of skeletal muscle begins with a motorneuron stimulating muscle fibers at their neuromuscular junction, where an action potential is triggered on the fiber cell membrane. Action potentials then propagate along the sarcolemma, as well as into the transverse tubules (t-tubules), which are invaginations of the sarcolemma. Action potentials are electrochemical events, consisting of a depolarization phase generated by Na^+ influx through voltage-gated Na^+ channels (Na_v), followed by a repolarization phase where K^+ effluxes from the cell through voltage-gated K^+ channels (K_v). Depolarization of t-tubular membranes activates L-type calcium channels, also known as dihydropyridine (DHP) receptors, causing them to undergo a conformational change. This in turn causes an interaction with the Ca^{2+} release channels of the sarcoplasmic reticulum (SR), known as the ryanodine receptors (RYRs), which allows the Ca^{2+} release into the sarcoplasm (Westerblad et al., 1991).

Skeletal muscle fibers contain sarcomeres, which are the functional unit for contraction. Upon increase in intracellular $[Ca^{2+}]$ ($[Ca^{2+}]_i$) Ca^{2+} binds to troponin C, causing a conformational change, removing tropomyosin away from the myosin binding sites on actin. The myosin cross-bridge then binds to actin, which then pulls the actin towards the center of the sarcomere, allowing muscle to do work and/or generate force. Finally, Ca^{2+} detaches from the troponin and is actively pumped back to the SR via Ca^{2+}-ATPases located on the SR membrane. This allows for relaxation.

Hyperkalemic periodic paralysis is a channelopathy caused by a defect in the $Na_{v1.4}$ channel, the Na_v isoform expressed in skeletal muscle. It is characterized by periods of

myotonic discharge, leading to episodic paralysis during which serum K^+ becomes elevated. The paralysis completely incapacitates patients, leaving them unable to move and sometimes bed-ridden, for a period of hours to days. Thus far, none of the available treatments are fully effective, and those that are available often become ineffective over time. The mechanism of the disease is not fully understood and before further treatments can be developed, we need to understand how mutations of the $Na_{v1.4}$ channel cause the HyperKPP symptoms.

One feature of the disease is that there is an asymptomatic period early in life followed by an increase in frequency of symptoms until adolescence. It is known that $Na_{v1.4}$ is expressed soon after birth, and reaches maximum content by the age of ten (Zhou & Hoffman, 1994). An answer to this question is important because it raises the possibility that muscles have a low density and/or low activity levels of defective $Na_{v1.4}$ channels or that there is a change in protein expression in other channels causing the symptoms (i.e. a change in fiber type from type I to IIA).

This work was carried out as part of a larger study that investigated the extent by which the mutant $Na_{v1.4}$ channel contributes to the HyperPP symptoms at different ages. For this study, a HyperKPP mouse model was used in which the equivalent human M1592V mutation had been knocked-in the mouse genome. The overall objective of this thesis was to focus on the progress of symptoms in EDL and soleus by measuring their contractile characteristics *in vitro* using HyperKPP mice between two weeks and twelve months of age.

MEMBRANE POTENTIALS

Membrane potential in all cells is determined by three factors: i) the concentration of ions on the intra- and extracellular side of the cell membrane ii) the permeability of these ions to the cell membrane and iii) the activity of electrogenic pumps that maintain these ion

concentrations (i.e. Na^+-K^+ ATPase).

Under normal conditions, concentration gradients are observed for all ions. For example, Na^+ and Cl^- concentrations are highest outside of the cell, while for K^+ the reverse is observed. Thus, there is a constant flux of these ions down their concentration gradient. At the same time there is a membrane potential in which the inside of the cell is more negative than the outside. According to the electrical gradient, Na^+ and K^+ move toward the inside of the cell, while Cl^- moves towards the outside of the cell. The membrane potential at which electrical and chemical gradients are perfectly balanced for a given ion is called the equilibrium potential (or reversal potential, E_{rev}); i.e. it is the potential at which there is no net flux from the ion. However, due to active ion pumps, none of Na^+, K^+ or Cl^- is at their respective equilibrium potentials. There is therefore a constant flux of ions across the cell membrane. The equilibrium potentials for K^+ (E_K), Cl^- (E_{Cl}) and Na^+ (E_{Na}) are respectively -90, -66 and +60 mV, in skeletal muscle (Begenisich & Cahalan, 1980). As each ion is trying to bring the membrane potential (Em) toward its own equilibrium, for a normal resting E_m of -80 mV there is a constant K^+ and Cl^-efflux and Na^+ influx. As a consequence of these fluxes, Na^+ and Cl^- ions tend to depolarize the cell membrane, whereas K^+ ions tend to hyperpolarize the membrane.

The greater the difference between E_m and E_{rev}, the greater the driving force for ion flux. From this point of view, Na^+ would be expected to cause more depolarization than K^+ and Cl^-. However, the contribution of an ion to E_m also depends on its permeability (P). In skeletal muscle at rest, the P_K:P_{Cl}:P_{Na} ratio is 1: 10: 0.005 (Adams et al., 1980). Despite the Em-E_{Na} being the largest, Na^+ has little effect on resting Em because its $Na_{v1.4}$ channels are closed. The same is not true for K^+ and Cl^- because some of their channels are opened

allowing for a modulation of E_m (Adams et al., 1980). The channel controlling Cl^- permeability at rest is the *CLC-1* chloride channel. For K^+, at least two channels are open at rest. Both are members of the K_{ir} superfamily of K^+ channels that have either strong or weak inward-rectifiers (Kubo et al., 1993). The strong-inward rectifying K^+ channel ($K_{ir2.1}$) is named for the fact that it has lower permeability for outward K^+ current than inward current (Fakler et al., 1995). The second K^+ channel is the ATP-sensitive K^+ channel (K_{ATP}), and is made up of two subunits. One subunit, Kir6.2, has the ATP binding site that closes the channel. The other subunit is the SUR2A subunit, (Seino et al., 1999) a member of the ATP-binding cassette (ABC) superfamily. This subunit has two nucleotide binding folds for ADP binding that cause the opening of the channels.

Action potentials are initiated when the membrane potential depolarizes to about -60 mV. At that Em, Na_v channels become activated, and Na^+ becomes the ion with the largest conductance. Na^+ becomes the dominant ion controlling E_m, causing the depolarization to -10 mV. To terminate the action potential, the Nav channels inactivate and P_{Na} decreases. Also, K_v channels open to allow K^+ to efflux from the cell, terminating the AP and repolarizing the sarcolemma back to the resting Em.

Another contributor to E_m is the Na^+-K^+ ATPase pump, which pumps three Na^+ ions into the extracellular space and two K^+ ions into the intracellular space. This maintains the Na^+ and K^+ concentration gradients while generating a net outward current of one positive charge contributing to resting membrane potential (Clausen, 1993).

Thus, resting membrane potential is dependent on the distribution of Na^+, K^+ and Cl^- ions across the cell membrane. The electrical and chemical forces for a given ion combine to become a single force, the electrochemical gradient, allowing for the movement of ions

across the cell membrane.

Channelopathies are a group of inherited diseases involving the dysfunction of an ion channel caused by gene mutations. The resulting defective channels greatly affect membrane excitability either by first acting on how the resting Em is controlled or directly on the generation of action potentials. These channelopathies leads to a spectrum of symptoms ranging from myotonia to periodic paralysis. Myotonia is characterized by membrane hyperexcitability, causing sustained contractions and an inability of muscle to relax. Myotonia is caused by mutations on the ClC-1 Cl^- or the $Na_{v1.4}$ Na^+ channels. At the other end of the spectrum, periodic paralysis is characterized by a complete loss of membrane excitability, which leads to periods of paralysis causing muscle weakness. For these channelopathies, the mutations are found on the $Ca_{v1.1}$, $Na_{v1.4}$ and $K_{ir2.1}$ channels. Some channelopathies have both symptoms, and both are due to mutations of the $Na_{v1.4}$ channels. To best understand these diseases, especially those linked to the $Na_{v1.4}$, the electrophysiological and molecular characteristics of the $Na_{v1.4}$ will first be discussed, followed by a full discussion on HyperKPP.

VOLTAGE-GATED Na^+ CHANNEL

Na_v channels are among the cation voltage-sensitive channels that are made of four membrane domains, each consisting of six transmembrane segments. They have three essential electrophysiological properties that are important for generation, propagation, and control of AP's. These properties are channel activation, fast inactivation, and slow inactivation.

Electrophysiological characteristics

According to the steady-state IV (current-voltage relationship) curve a Na^+ current

starts to be observed when the membrane is depolarized to -60 mV (Chahine et al., 1994; Kontis et al., 1997) (Fig. 1). However, in the resting state addition of TTX (a Na^+ channel blocker) causes a slight hyperpolarization (Yensen et al.,2002). When $[K^+]_e$ is changed the membrane potential depends primarily on $[K^+]_e$ when above 10 mM. Below 10 mM, Em was always less than the expected value from the Nernst potential and this deviation was explained if a small Na^+ permeability was taken into consideration, being 1% of the K^+ permeability (Hodgkin & Katz, 1949). Together these results indicate that a few $Na_{v1.4}$ channels are open at resting E_m of -80 to -70 mV, but the open probability of Na_v channels is extremely low, and too few channels are open to be able to measure a current. At a membrane potential of -30 mV, half of the sodium channels are activated, and maximum current occurs at -10 mV (Ji et al., 1996) (Fig. 3).

The channels open for less than a millisecond, allowing Na^+ to enter the cell down its concentration gradient, causing a macroscopic current that rises to its peak within less than a millisecond (Fig. 2). Current then begins to decrease as Na^+ channels begin to fast inactivate, while E_m is still depolarized. The steady-state fast IV curve for fast inactivation shows that channels begin to fast inactivate around -70 mV, and is fully fast inactivated at -40 mV (Fig. 3). Fast inactivation functions to terminate the action potential and repolarize the sarcolemma. It is also responsible for creating a refractory period, allowing for unidirectional propagation of the AP, preventing the AP from backward propagation.

$Na_{v1.4}$ channels have a second type of inactivation that occurs on a time scale of seconds to minutes. This type of inactivation is called slow inactivation as opposed to the fast inactivation discussed above. It appears to be a separate voltage-dependent process, which acts to modulate the number of available Na^+ channels on the cell membrane. Slow

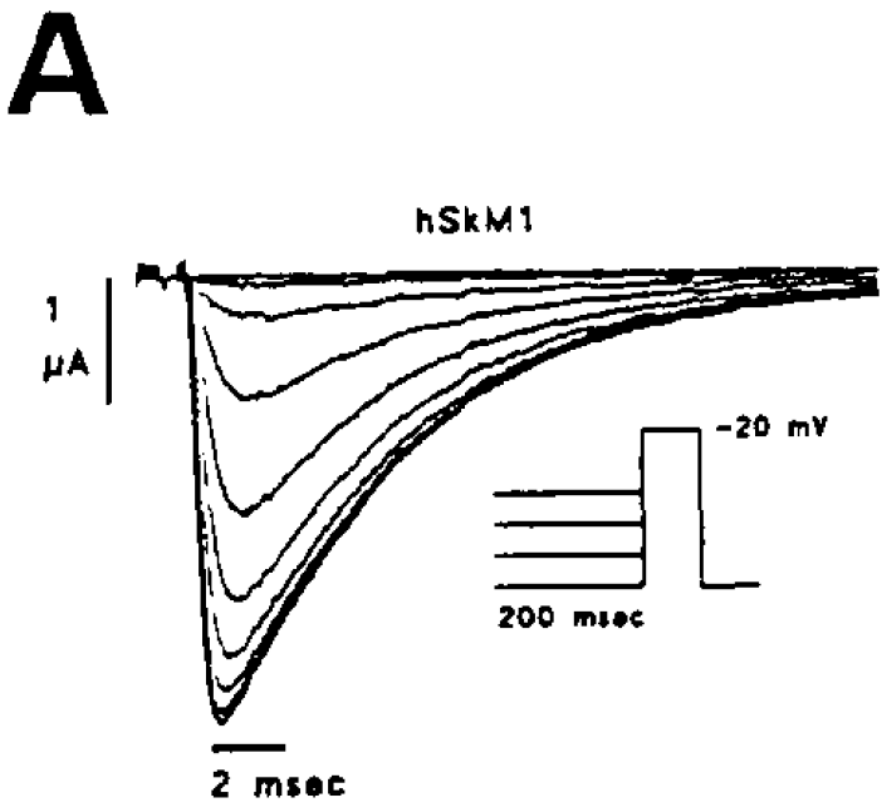

Figure 1. Na^+ current trace. A family of currents recorded from *Xenopus* oocytes expressing hSkM1, in response to a series of voltage steps (-80 to +10 mV) from a holding potential of -100mV (Figure and legend from Makita et al., 1994).

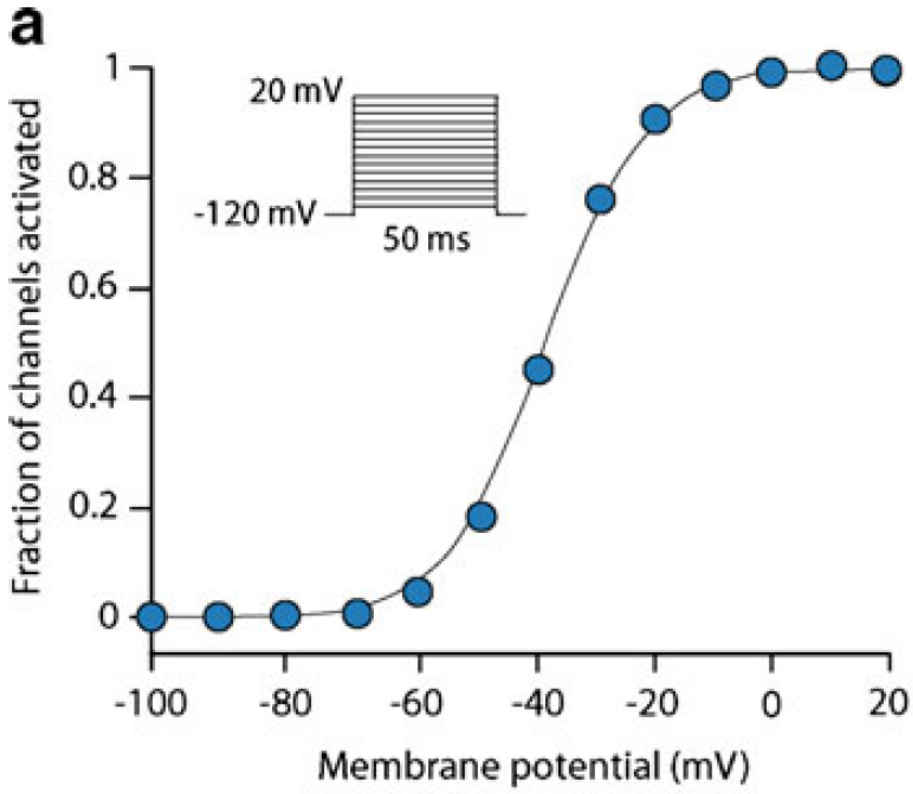

Figure 2. Voltage-dependent activation of the sodium channel. Using a patch-clamp technique, the membrane potential dependence of activation is studied by applying 50 ms depolarizing voltage steps from a holding potential of -120 mV (inset) (Figure and legend from Amin et al., 2010).

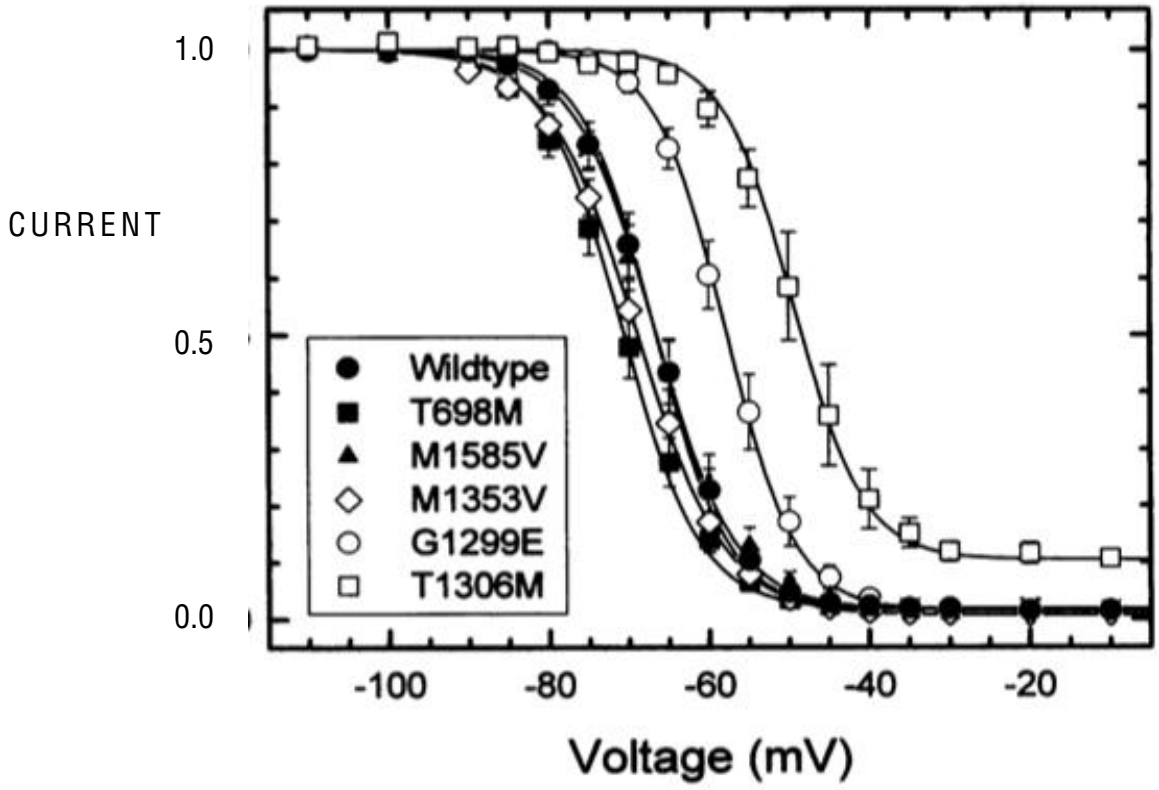

Figure. 3. Voltage dependence of fast inactivation. Channel availability was measured as the peak Na^+ current elicited by depolarization to -10 mV, after a conditioning pulse at potentials of -140 to -10 mV. Amplitude was normalized to the current after a conditioning pulse at -140 mV. The voltage dependence of steady-state fast inactivation was measured using a fixed 300-ms conditioning pulse. Symbols depict the means ± SEM (Figure and legend from Hayward et al., 1997).

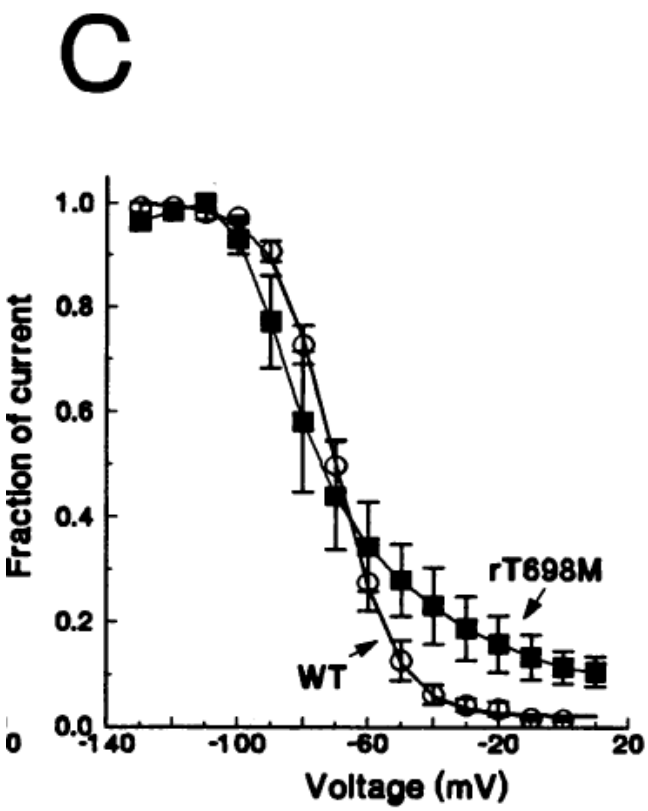

Figure 4. Steady-state slow inactivation curve. The steady-state slow inactivation (s_∞) curves for WT and rT698M cells are shown. Cells were held at potentials starting from -130 mV and increasing to +10 mV in 10-mV steps. After 50 s at each holding potential, a 10-ms recovery pulse to -100 mV and a 20-ms test pulse to -10 mV were given before the holding potential was incremented. The peak current elicited by the test pulse to -10 mV is plotted as a fraction of the maximum current for WT cells and rT698M cells. The value of s_∞ remains large even at positive potentials, indicating that slow inactivation is impaired in rT698M cells. The peak current elicited by the test pulse to -10 mV is plotted as a fraction of the maximum current for WT cells and rT698M cells. (Vs = -70.3 mV). (Figure and legend from Cummins & Sigworth, 1996)

inactivation causes a decrease in Na^+ channel amplitude during subsequent depolarizations due to a decrease in channel availability (Cummins et al., 1996). Under steady-state conditions, none of the $Na_{v1.4}$ channels are slow inactivated between -120 mV and -100 mV. Half the channels are half-inactivated at -70 mV. By -20 mV, 95% of $Na_{v1.4}$ channels are slow inactivated (Hayward et al., 1999) (Fig.4).

Molecular structure

Na_v channels are composed of at least two protein subunits, the α and β subunits. The α-subunit forms the pore of the channel, and contains all functional components; that is, it controls activation, fast and slow inactivation. The β subunit modulates the channel activity. The Na_v α subunit constitutes a superfamily of ten genes encoding for $Na_{v1.1}$-$Na_{v1.9}$ and the β subunit contains four genes encoding for β1- β4 (Kallen et al., 1990; Rogart et al., 1989; Schaller et al., 1995) (Table 1 & Table 2).

Skeletal muscle expresses two α isoforms. The $Na_{v1.5}$ is the main Na^+ channel during development and its content is still very high at birth. $Na_{v1.4}$ channels are barely expressed in skeletal mouse sarcolemma at birth. $Na_{v1.4}$ protein content increases during the first days of postnatal development. In mouse, $Na_{v1.5}$ completely disappears by 20 days postnatal, while $Na_{v1.4}$ reaches its maximum content by 30 days. In humans, $Na_{v1.4}$ reaches its maximum content much later, being around ten years of age (Zhou & Hoffman, 1994).

The *SCN4A* gene encodes for the $Na_{v1.4}$ channel and is located on chromosome 17q23-25. In skeletal muscle, the $Na_{v1.4}$ channel is a heteromeric integral membrane protein, containing a 260 kDa α-subunit (Kraner et al., 1989). The α-subunit is composed of 1836 amino acid residues. Through hydropathy analysis, the proposed topology includes four domains (numbered I-IV), each one containing six α-helical transmembrane segments

PROTEIN NAME	GENE	EXPRESSION PROFILE
$Na_{v1.1}$	*SCN1A*	Central neurons, peripheral neurons, cardiac myocytes
$Na_{v1.2}$	*SCN2A*	Central neurons, peripheral neurons
$Na_{v1.3}$	*SCN3A*	Central neurons, peripheral neurons, cardiac myocytes
$Na_{v1.4}$	*SCN4A*	Skeletal muscle
$Na_{v1.5}$	*SCN5A*	Cardiac myocytes, uninnervated skeletal muscle, central neurons, fetal myocytes
$Na_{v1.6}$	*SCN8A*	Central neurons, dorsal root ganglia, peripheral neurons, heart, glia cells
$Na_{v1.7}$	*SCN9A*	Dorsal root ganglia, sympathetic neurons,
$Na_{v1.8}$	*SCN10A*	Dorsal root ganglia
$Na_{v1.9}$	*SCN11A*	Dorsal root ganglia
Na_{vx}	*SCN7A*	Heart, uterus, skeletal muscle, astrocytes, dorsal root ganglia cells

Table 1. Overview of voltage-gated sodium channel family (Yu & Catterall, 2003).

PROTEIN	GENE	ASSEMBLES WITH	EXPRESSION PROFILE
$Na_v\beta1$	*SCN1β*	$Na_{v1.1}$ to $Na_{v1.7}$	Central neurons, peripheral neurons, skeletal muscle, heart, glia
$Na_v\beta2$	*SCN2β*	$Na_{v1.1}$, $Na_{v1.2}$, $Na_{v1.5}$ to $Na_{v1.7}$	Central neurons, peripheral neurons, heart, glia
$Na_v\beta3$	*SCN3β*	$Na_{v1.1}$ to $Na_{v1.3}$, $Na_{v1.5}$	Central neurons, adrenal gland, kidney, peripheral neurons
$Na_v\beta4$	*SCN4β*	$Na_{v1.1}$, $Na_{v1.2}$, $Na_{v1.5}$	Heart, skeletal muscle, central neurons, peripheral neurons

Table 2. Nomenclature and some functions of voltage-gated sodium channel beta subunits (Catterall et al., 2003).

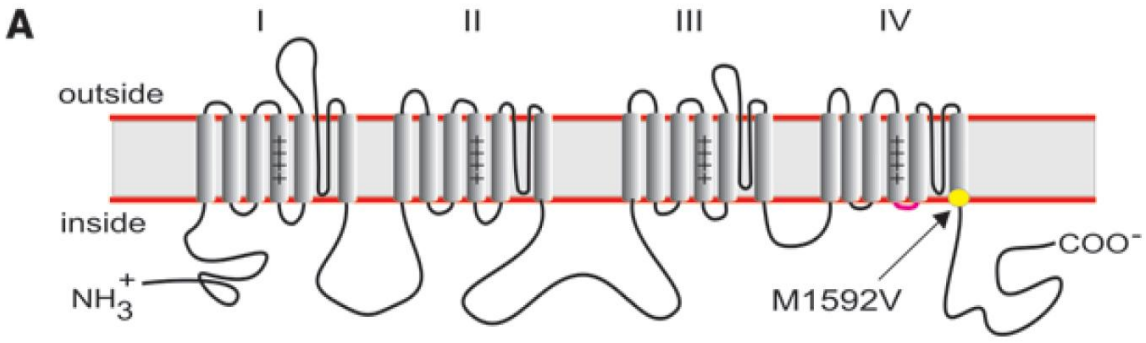

Figure 5. Na^+ channel structure. Na^+ channel topology and the location of the Met1592Val substitution within the S6 segment of domain IV (figure and legend from Hayward et al., 2008).

(numbered 1-6) (Kyle, 2007) (Fig. 5).

Spans 1-3 contain hydrophobic amino acids, and as a consequence of their composition, these three spans interact and anchor the channel in the membrane lipid bilayers. The fourth transmembrane segment of each domain contains 5-7 positive charges from lysine or arginine residues at every third position, and is thought to act as the voltage sensor of the channel (Noda et al., 1984). This was supported by experiments that have been performed in which individual residues at S4 were mutated by replacing the positive lysine or arginine charges with neutral charges. This resulted in a large shift in the voltage dependence of activation in the depolarizing direction (Kontis et al., 1997; Stuhmer et al., 1989). While the mechanism is still not clearly understood, it is thought that the S4 segment actually physically moves through the membrane, inducing a conformational change that allows opening of the pore. The external charges become exposed on the outer surface of the membrane, and the inner charges remain inside the membrane (Patton et al., 1994). Spans 5 and 6 contain the selectivity barrier for the Na^+. They are linked by a hairpin extracellular loop and line the pore of the channel (Jurkatt-Rott et al., 2007). The residues implicated in Na^+ selectivity are the negatively charged glutamic acid and aspartic acid, as well as the positively charged lysine. These negative amino acids function to attract the positively charged Na^+ ion, and to keep out the negatively charged Cl^- ion. The cations flow into a more constricted part of the pore, which is too small for the large K^+ ion to fit through (Jurkatt-Rott et al., 2007).

The cytosolic linker between domains III and IV plays a key role in the fast inactivation process, involving the binding of a cytoplasmic particle to its receptor (Armstrong et al., 1973). The linker has a unique hydrophobic sequence of three amino acids,

isoleucine, methionine and phenylalanine, known as the IMF motif. This motif blocks binds to the inner mouth of the pore, where it mediates fast inactivation (Stuhmer et al., 1989). Mutations predominantly causing myotonia, such as T1306M and M1353V, within the linker of repeats III-IV reduces fast inactivation activity, while slow inactivation activity is preserved (Cummins et al., 1996). Furthermore, it was shown that mutations causing prominent myotonia showed a shift in voltage dependence of steady-state inactivation towards less negative (Fig. 3) (Hayward et al., 1997). The cytoplasmic end of S6 in domain IV has been shown experimentally to contribute to the inactivation gate receptor (Cannon et al., 1993).

It has been determined that slow inactivation is a separate process, which does not involve the III-IV linker inactivation particle. The mechanism of slow inactivation is still not fully understood. Mutations at the cytosolic ends of S5 and S6, which form the inner mouth of the pore, have been shown to disrupt slow inactivation, suggesting that the slow inactivation process may involve a conformational change at the inner mouth of the channel (Hayward et al., 1997).

Beta-subunit

In skeletal muscle, only one β subunit is associated with the $Na_{v1.4}$ channel. A single gene encodes the 38 kDa β-subunit, and is located on chromosome 19. The subunit consists of a single transmembrane domain with an extracellular N terminus and an intracellular C terminus, and tends to be heavily glycosylated. It enhances the Na^+ current amplitude 2.5-fold, causes a 5-fold acceleration in the kinetics of sodium channel inactivation and causes a 19 mV hyperpolarizing shift in steady state inactivation (Patton et al., 1994; Zhou et al., 1991). It is thought that these multiple events may result from molecular interactions

between the α and –β subunit, or from a single molecular mechanism that alters several aspects of Na_v channel function (Patton et al., 1994; Wallner et al., 1993). Thus far, the β-subunit has not been linked to any human disease (Messner et al., 1985; Reber et al., 1987).

$Na_{v1.4}$ MUTATIONS

Channelopathies are a group of inherited diseases involving the dysfunction of an ion channel caused by gene mutations, leading to a spectrum of symptoms ranging from myotonia to periodic paralysis (Fig.6). Myotonia congenita is caused by a reduced sarcolemmal Cl^- conductance (g_{Cl}) due to mutations in the gene encoding the skeletal muscle Cl^- channel (CLC-1), causing membrane hyperexcitability (Fahlke et al., 1997). Potassium-aggravated myotonia is caused by a defect in the fast inactivation process of the $Na_{v1.4}$ channel. Myotonia occurs when Na_v channels open uncontrollably, which is aggravated by K^+ ingestion, especially when increased K^+ causes depolarization of the cell membrane (Kubota et al., 2009). At the other end of the spectrum, periodic paralysis is characterized by a complete loss of membrane excitability, which leads to periods of paralysis causing muscle weakness. Hypokalemic periodic paralysis (HypoKPP) is an example of periodic paralysis due to mutations of either the $Na_{v1.4}$ and $Ca_{v1.1}$ channels, the latter being the channel containing the dihydropyridine receptors and ryanodine receptors. HypoKPP is associated with low serum potassium levels, which appears to trigger the paralysis by causing $K_{ir2.1}$ and $K_{ir6.2}$ channels to malfunction, leading to large depolarizations, which cause acute attacks of muscle weakness (Jurkatt-Rott et al., 1994 &2000). Another disease causing periods of episodic paralysis is Andersen-Tawil Syndrome. It is caused by mutations in the $K_{ir2.1}$ channel, causing periodic paralysis in skeletal muscle, arrhythmias in cardiac muscle, and dysmorphic features (Zhang et al., 2005).

Paramyotonia congenita (PC) and hyperkalemic periodic paralysis (HyperKPP) are distinguished from other channelopathies, as patients exhibit a combination of both myotonia and periodic paralysis. Both are related to defects of the $Na_{v1.4}$ channel.. While HyperKPP is sensitive to increases in serum potassium, PC is not. Furthermore, PC can be distinguished from HyperKPP in that patients experience a paradoxical worsening of symptoms upon muscle cooling (Ptacek et al., 1991). PC patients typically show symptoms of muscle stiffness or myotonia, caused by membrane hyperexcitability. Conversely, the dominant clinical presentation of symptoms in HyperKPP patients is episodic weakness or paralysis, caused by sarcolemmal inexcitability when extracellular $[K^+]$ increases (Yang et al., 1994).

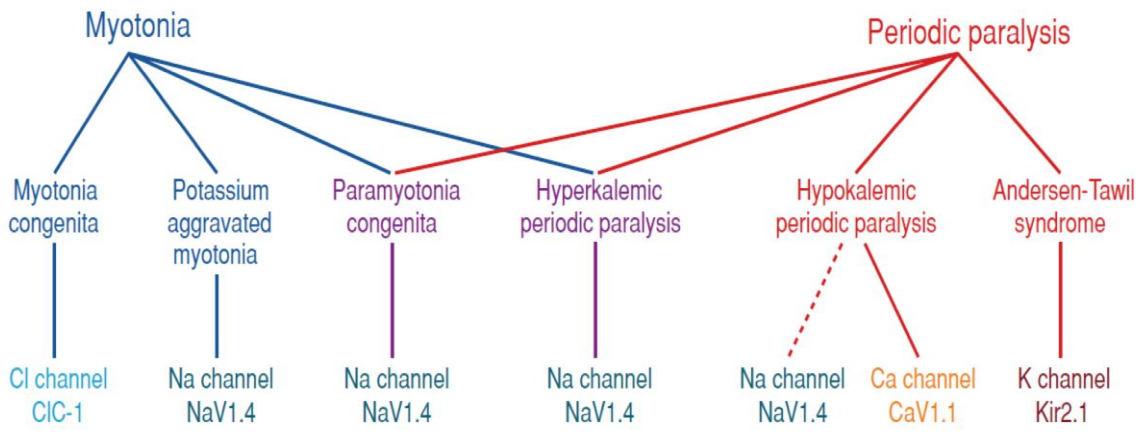

Figure 6. Clinical spectrum of the nondystrophic myotonias and periodic paralyses. Myotonia predominates in disorders further to the left in this spectrum, whereas periodic paralysis is the major symptom for those to the right. The underlying molecular genetic defects in each of these disorders are mutations in voltage-gated ion channel genes (*middle row).* (Figure and legend taken from Cannon, 2006).

HYPERKALEMIC PERIODIC PARALYSIS

Symptoms

This autosomal dominant ion channelopathy has an almost complete penetrance, and is one of several familial disorders of impaired muscle excitability caused by a missense mutation in the skeletal muscle Na^+ channel $Na_{v1.4}$.

The hallmark features of HyperPP are an increase in $[K^+]_{plasma,}$ from the normal 4 mM up to 8 mM, although in many instances K^+ increases to 6.0-6.5 mM (Gamstrop et al., 1957; Lehmann-Horn et al., 2007). In the early stages of the disease, periods of myotonic discharge occur, during and between paralytic attacks, causing weakness (Lehmann-Horn et al., 2007). The duration of the attacks varies between and within patients and can last from a few hours to days, with extreme cases lasting several months (Bradley et al., 1990; Miller et al., 2004; Pearson et al., 1964). Patients may suffer the first paralytic attack at 6 months of age, but in general 44% of patients have the first attack prior to the age of five, and 92% before the age of ten (Gamstrop et al., 1957; Jurkatt-Rott et al., 2007). Intervals between attacks can last several days but in many cases patients experience one to three attacks per day. The attacks tend to be short and frequent in childhood, but become longer and more severe during adolescence (Bradley et al., 1990; Gamstrop et al., 1957; Lehmann-Horn et al., 2007; Pearson et al., 1964).

The predominant symptom of HyperPP is weakness, occurring particularly in the limb muscles, and generally spares extraocular muscles (Bradley et al., 1990; Gamstrop et al., 1957). Other tissues, such as cardiac muscle and neurons, are not affected by mutations of the *SCN4A* gene because they express other Na_v isoforms; i.e. cardiac muscle expresses $Na_{v1.5}$, while neurons express $Na_{v1.1}$-$Na_{v1.3}$ and $Na_{v1.6}$-$Na_{v1.9}$ (Goldin et al., 2000; Kyle et al.,

2007). Interestingly, except for two reported cases, HyperKPP patients do not suffer from respiratory distress, despite the fact that the diaphragm, a major respiratory muscle, expresses $Na_{v1.4}$ (Zhou et al., 1994).

As patients approach the age of 30, the paralytic attacks and myotonic discharge usually cease. However, they may experience a debilitating muscle myopathy, making tasks such as walking difficult. Other characteristics of later-stage HyperPP include fiber damage, large number of fibers containing central nuclei, suggesting significant fiber regeneration and vacuolar myopathy (Hayward et al., 2008; Pearson, 1964; Streeten et al., 1971). A shift in fiber type composition towards a more oxidative phenotype typically occurs as an effect of repetitive muscular activity produced by chronic contractions. Furthermore, it has been suggested that the decrease in force generation that occurs with age may be related to the amount of fiber damage that takes place in earlier years (Bradley et al., 1990; Miller et al., 2004).

Mutations of the alpha subunit

Of the nine mutations associated with HyperKPP, T704M and 1592V, each correspond to 33% of affected patients, while the other 33% are due to the seven remaining mutations (Miller et al., 2004) (Fig. 7). However, the range of onset, frequency, duration and severity varies not only between mutations but also within patients having the same mutation. The average age of onset for the T704M mutation is around eight months old, ranging from 0 to 9 months, whereas the M1592V mutation does not tend to begin affecting patients until five years of age, with a range of 0 to 10 years. The other seven mutations begin around the age of two on average, and range from 0-16 years of age. The frequency of attacks for the T704M mutation occurs between 8 to 42 attacks per month, with the frequency is much less

for the M1592V mutation, being 5-6 attacks per month. However, the mean duration of the paralysis is about ten times longer for the M1592V mutation than for the T704M (89 hours vs. 8 hours), with the maximum duration as long as seven days for both mutations. For the other seven HyperKPP mutations, the average age of onset is two years of age, with the frequency of attacks ranging from 1-42. The average duration of these attacks is 24 hours, with a range of 2-72 hours (Miller et al., 2004).

Triggers

Ingestion of KCl consistently triggers an attack in all HyperKPP patients but not in normal individuals, suggesting that HyperKPP patients have a greater sensitivity to increased extracellular [K^+] (Bradley et al., 1990; Gamstrop et al., 1957). The most common and consistent trigger for a paralytic attack is a period of about one hour of rest after exercise (Bradley et al., 1990; Lehmann-Horn et al., 2007; Pearson et al., 1964). A paralytic attack will occur after this rest period 70-80% of the time in all HyperKPP patients.

Furthermore, the more intense the exercise, the more intense the paralytic attack. Other less consistent triggers include exposure to cold, emotional stress, and periods of fasting (Lehmann-Horn et al., 2007; Miller et al, 2004). Paralysis is triggered more easily by cold (58%) and stress (46%) in patients with the T704M mutation whereas patients with the M1592V mutation are less sensitive to cold (38%) and stress (13%) (Miller et al., 2004).

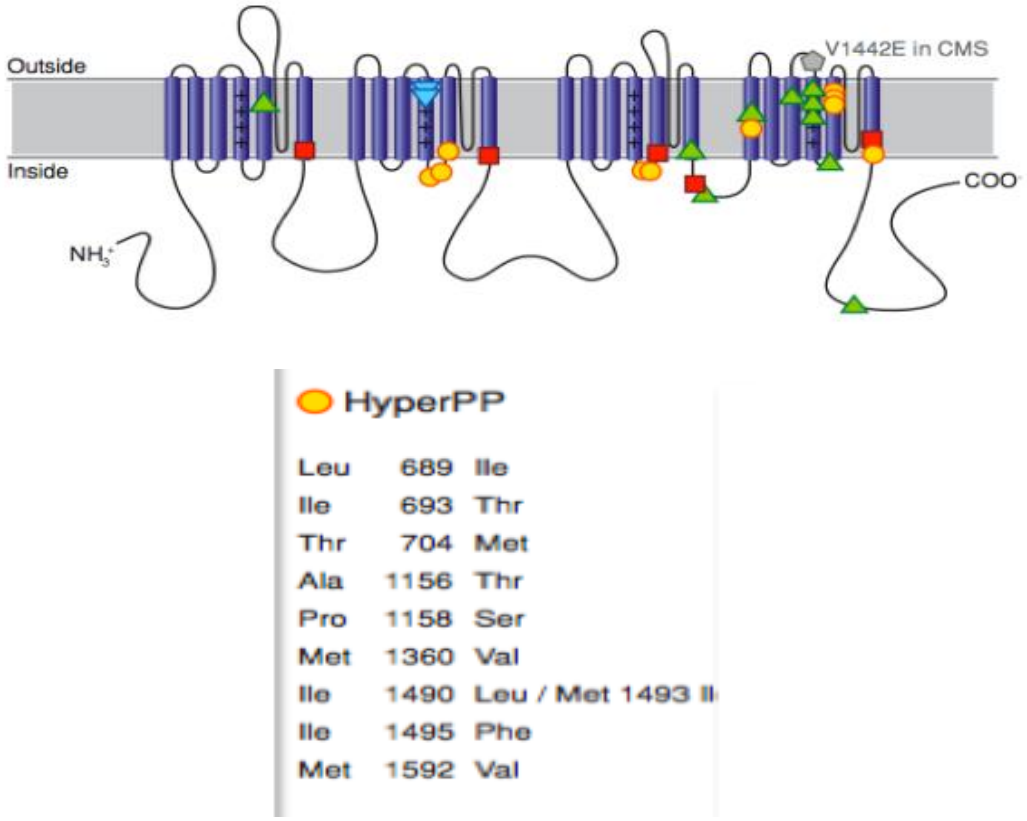

Figure 7. Missense mutations in $Na_{v1.4}$ associated with Hyperkalemic periodic paralysis. The schematic diagram from the membrane-folding structure of $Na_{v1.4}$ shows the relative locations of missense mutations associated with hyperkalemic periodic paralysis (HyperPP) (Figure and legend from Cannon, 2006).

Treatments for HyperKPP

Often patients will experience a "creeping" sensation in their legs prior to the onset of a paralytic attack. Attacks can be prevented by low-intensity exercise, such as walking. This is an interesting paradox because mild exercise causes an increase in $[K^+]_e$, from 4 mM to 8-11 mM yet it prevents paralysis under these conditions (Bradley et al., 1990; Jurkatt-Rott et al., 2007; Lehmann-Horn et al., 2007). It has been shown that daily use of carbonic anhydrase inhibitors, such as acetazolamide, limits the frequency of attacks, and calcium gluconate helps to alleviate the severity of the attacks. Furthermore, during an attack, inhaled β-adrenergic agonists, such as Salbutamol, help to alleviate symptoms (Clausen et al., 1980 & Wang et al., 1976). Salbutamol (10^{-7} M) has been shown to fully restore tetanic force in HyperKPP soleus; however, long-term use of Salbutamol has been shown to cause adverse changes in lung function, and becomes ineffective over time (Clausen et al., 2011).

Electrophysiology of mutant $Na_{v1.4}$ channels

Several groups have studied the T704M mutation and two different mechanisms have been proposed: Using the rat homolog T698M mutation (rT698M), Cummins et al. (1993) found that the activation voltage dependence was shifted in the hyperpolarizing direction by 10-15 mV relative to wild-type channels. When the steady-state activation and inactivation curves are then plotted on the same graph, the shift increases the area under the curves where they cross-over, resulting in a greater "window" currents between -75 and -40 mV (Cummins et al., 1993). In another series of experiments by Cummins et al. (1996), a defect of slow inactivation for the T704M mutation was shown after a prolonged depolarization at -20 mV, where 97% of wild-type channels were slow inactivated, compared to only 75% of mutant channels. The T704M and M1592V mutations do not affect the kinetics of fast inactivation

(Hayward et al., 1999). Instead, these mutations affect the slow inactivation process. Under steady state conditions, none of the $Na_{v1.4}$ channels are slow inactivated at -120 mV while 50% are inactivated at -70 mV. By -20 mV, 95% of wild type channels are slow inactivated. T704M and M1592V channels exhibit impaired slow inactivation at voltages less negative than -60 mV. Only 65% of channels are inactivated at -20 mV for both mutations. Furthermore, the rate of onset for slow inactivation is significantly slow, while recovery from slow inactivation is faster for T704M and M1592V channels compared to normal channels (Hayward et al., 1999).

Physiology of HyperKPP skeletal muscles

Defective slow inactivation results in the opening of Na^+ channels in the resting state. The subsequent membrane depolarization associated with the Na^+ influx then causes generation of uncontrolled APs, i.e., APs spontaneously generated without a proper trigger, leading to myotonic discharges (Cannon et al., 1993). The K^+ efflux associated with APs causes an increase in interstitial $[K^+]$, $[K^+]_{plasma}$ and t-tubular $[K^+]$ (Lehmann-Horn et al., 2007). A common feature of HyperKPP muscles is an increased sensitivity to elevated $[K^+]_e$. An increase in $[K^+]_e$ from 3.5 to 7 mM causes large membrane depolarization of about 30 mV in HyperKPP muscles compared to only 10 mV in wild-type (Cannon et al., 1991). Furthermore, the excessive depolarization is associated with an abnormal Na^+ influx that increases intracellular $[Na^+]$. The addition of tetrodotoxin (TTX) prevents the excessive depolarization at increased $[K^+]$ as a result of the Na^+ influx. Once the depolarization becomes great enough to inactivate a large number of Na^+ channels, paralysis occurs (Lehmann-Horn et al., 2007). Abnormal increases in intracellular $[Na^+]$ have also been reported in HyperKPP muscles when $[K^+]_e$ increases (Jurkatt-Rott et al., 2007). Thus, the

increase in $[Na^+]_i$, which results from the Na^+ influx, is another factor contributing to paralysis.

For HyperPP patients, a treatment involving blocking of $Na_{v1.4}$ channels using pharmacological agents is not possible without causing death. The next approach is then a modulation of other ion channel activity to prevent the Na^+ induced depolarization and K^+ - induced paralysis. However, several questions about the mechanism of the disease are not fully understood and before further treatments can be developed, we need to understand how mutations of the $Na_{v1.4}$ channel causes all of the symptoms. Two of these questions are the subject of this thesis. That is:

1. Why is there an asymptomatic period early in life?
2. Why is there an increase in frequency of symptoms with age?

Those two questions are important because it raises the question as to whether all symptoms are related solely to the $Na_{v1.4}$ channels, or whether some symptoms starts with the defective $Na_{v1.4}$ channels, while other symptoms are due to changes in gene expression. It has been shown by Hayward et al. (2008) that EDL from HyperKPP mice exhibited changes in fiber type to a more oxidative phenotype, as well as upregulation of the transcriptional coactivator PGC-1α. Another study showed that cells exposed to high $[K^+]_e$ became depolarized to values at which excitatory Na^+ current is normally inactivated, which was due to an increased Na^+ conductance (Lehmann-Horn et al., 1983).

OBJECTIVES AND HYPOTHESIS

To answer the above two questions, a large study was undertaken to examine the extent by which mutant Na^+ channels contribute to HyperPP symptoms at different ages; i.e. to follow how the disease progresses, in relation to changes in $Na_{v1.4}$ content. The specific

objective of this M.Sc. study was to follow changes in contractile characteristics of EDL and soleus muscles from mice between the ages of 2 weeks and 12 months. Both muscles were used because 1) they have different fiber type compositions (EDL is primarily composed of type IIB and IIX fibers, whereas the soleus is composed of type I and IIA fibers (Banas et al., 2011; Thabet et al., 2005) and 2) to determine if different fiber type composition give rise to differences in symptoms. The hypothesis of this thesis is that some symptoms start with the defective $Na_{v1.4}$ channels, while other symptoms start after some changes in gene expression affecting membrane channel content and/or activity.

CHAPTER 2

METHODS AND MATERIALS

METHODS

Animals

HyperKPP mice were generated by knocking in the equivalent human missense mutation M1592V in the genome of FVB1N mice; that is a mutation of methionine to valine at position 85 (Hayward et al., 2008). Mice were received from Dr. Lawrence Hayward at the University of Massachusetts Medical School, Worcester, Massachusetts. The homozygous mutants do not survive past postnatal day five (Hayward et al., 2008), and cannot be used. So, new HyperKPP mice were generated by crossbreeding heterozygous HyperKPP mice with FVB mice. To start a colony of wild type and HyperKPP mice, FVB1N mice were initially purchased (Charles River Laboratories, Canada) to crossbreed with the HyperKPP mice. All wild type and HyperKPP mice used in this study were those obtained by continuously cross-breeding FVB and HyperKPP mice. All mice were fed *ad libitum* and housed according to the guidelines of the Canadian Council for Animal Care (CCAC). The Animal Care Committee of the University of Ottawa approved all experimental procedures used in this study. Prior to muscle excision, animals were anaesthetized with a single intraperitoneal injection of 2.2 mg ketamine/0.4 mg xylazine/0.22 mg acepromazine per 10 g of animal body weight, and sacrificed by cervical dislocation.

Genotyping

DNA Extraction. All animals used in this study were genotyped using a piece from the tail. A 0.5-mm tail segment was lysed by incubation overnight with 500 uL lysis reagent (0.2 mM disodium EDTA and 25 mM NaOH, pH 12.31) and 50 uL Proteinase K (1 mg/ml) at 56°C. A volume of 650 uL of 1:1 Phenol:CIA was added to each tube and centrifuged at 12,

000 *g* for 10 minutes at room temperature. The upper phase was extracted with 650 uL of CIA to remove the phenol, vortexed for 10 seconds, and centrifuged for 10 minutes. The upper aqueous phase was mixed with 750 uL of isopropyl alcohol, incubated at room temperature for 10 minutes, and centrifuged at 12 000 *g* for 10 minutes. The pellet was washed with 750 uL of 70% ethanol and centrifuged for 10 minutes at 12 000 *g*. The DNA pellet was air dried for 30 minutes and suspended in 200 uL 1X TE buffer (10 mM Tris, 1 mM EDTA, pH 8.0), and allowed to incubate for two hours at 65°C.

PCR. For the PCR, the template primers were mSk757F, 5'TACTACTTCACCATTGGCTGGATATCTTCGACTTCG-3' at the 3' end of exon 23 and mSk998R, 5'CTGAGCACAATCTCCATTTCCCTCAGC-3' in the 3'-UTR of exon 24. 100 ng genomic DNA was added to a mixture of 2X Phusion Master Mix with GC Buffer (0.04 U/uL Phusion DNA polymerase, 2X Phusion GC Buffer, 400 uM of each dNTP and 100% DMSO (2 x 500 uL)). This produced a 1.43-kb DNA product amplified only from cDNA that was digested with NspI.

Physiological solutions for muscle tested *in vitro*

Soleus and EDL muscles were dissected (unless otherwise specified) in the control physiological saline solution. The control solution contained (in mM): 118.5 NaCl, 4.7 KCl, 2.4 $CaCl_2$, 3.1 $MgCl_2$, 25 $NaHCO_3$, 2 NaH_2PO_4, and 5.5 D-glucose. Paired muscles were used where one muscle was constantly superfused in the control solution and the other in a physiological solutions in which $[Ca^{2+}]_e$ was only 1.3 mM by reducing the appropriate amount of CaCl2. In some experiments, muscles were exposed to 4.0 mM Ca^{2+} by adding the appropriate amount of CaCl. Solutions containing 10 or 11 mM K^+ were made by adding the proper amount of KCl to the physiological solutions described above. All solutions were

continuously bubbled with 95% O_2–5% CO_2 to maintain a pH of 7.4. Experimental temperature was 37°C, unless otherwise indicated.

Force Measurement

Muscles were positioned horizontally in a plexiglas chamber containing 5 mL of solution. One end of the muscle was attached to a force transducer (Model # 40A, Aurora Scientific, Canada), while the other end was fixed to a stationary hook. The flow of physiological solution below and above muscles was maintained at a total of 15 ml/min. Muscle length was adjusted to give maximal tetanic force. Force transducers were connected to a KCP13104 data acquisition system (Keithley, USA) and data were recorded at 5 kHz. Parameters of the tetanic contraction were then later analyzed with a computer. Maximum tetanic force was defined as the maximal force measure at the beginning of each experiment after the length had been adjusted. Thereafter, peak tetanic force was measured as the maximum force during a stimulation subsequent to the maximum force. Both maximum and peak tetanic force were calculated as the difference between the maximum force during a contraction and the baseline force measured 5 ms before a stimulation. Unstimulated force, defined as the amount of force exerted by a muscle without stimulation, was calculated as the difference in baseline and zero force. Half relaxation was defined as the time required for the force to decrease from 95% to 50% of peak force after the last contraction in a train (Verburg et al., 2001).

Stimulation protocol

Electrical stimulations were applied across two platinum wires (4 mm apart) located on opposite sides of the fibers. They were connected to a Grass S88 stimulator and a Grass SIU5 isolation unit (Grass Technologies/Astro-Med Inc.). Tetanic contractions were elicited

with 200 ms trains of 0.3 ms, 12 V (supramaximal voltage) pulses. Stimulation frequencies for soleus and EDL were respectively 140 and 200 Hz. For all experiments, tetanic contractions were elicited every 100 s.

Experimental protocol

The first part of every experiment consisted in lengthening muscles for maximum force and in verifying that the stimulation voltage was at least 5-times that of the threshold voltage, defined as the smallest voltage to trigger a contraction. Once maximum tetanic force was obtained, the waveform was saved to obtain the maximum tetanic force as described above. All wild type muscles were then equilibrated for 30 minutes to ensure that the muscle remained stable. For wild type mice, muscles were not used if the drop in peak tetanic force was greater than 10% as for previous experiments in this laboratory (Gong et al., 2000; Cifelli et al., 2007). For HyperKPP muscles, it was not always possible to wait a full 30 min because many were unstable (see results for examples and details).

Statistical analysis

Data are presented as means ± S.E. Split plot ANOVA was used to determine significant differences. Split plot designs were used because muscles were tested at all time, K^+ or Ca^{2+} levels. ANOVA calculations were made using the version 9.2 GLM (General Linear Model) procedures of the Statistical Analysis Software (SAS Institute Inc., Cary, NC, USA). When a main effect or an interaction was significant, the least square difference (LSD) was used to locate the significant differences (Steel & Torrie, 1980). The word ‘significant' refers only to a statistical difference ($P < 0.05$).

CHAPTER 3

RESULTS

All experiments started with gradually increasing stimulation strength and muscle length until peak force elicited by electrical stimulations no longer increased; this period was defined as the maximization period. For wild type, peak tetanic force increased gradually until it reached a maximum force (Fig. 3-1A). This period was followed by a 30-minute equilibrium period to ensure that muscles were stable. During the equilibrium period, force decreased slightly, and muscles were discarded if force decreased by more than 10% (Matar et al., 2000). For EDL, the K^+ challenge consisted of exposing EDL to 11 mM K^+ for 60 min (as opposed to 4.7 mM in control conditions). For one muscle, an increase in $[K^+]_e$ caused a 27% decrease in tetanic force, which recovered to 90% when $[K^+]_e$ was returned to 4.7 mM (Fig. 3-1B). It is important to notice that for wild type EDL the baseline remained stable during the entire experiment.

For HyperKPP EDL muscles, the situation was very different. Some HyperKPP EDL had changes in tetanic force during maximization, equilibrium, and exposure to 11 mM K^+ that were very similar to that of wild type EDL (Figure 3-2A). Other HyperKPP EDL had an unstable baseline, representing the force measured between contractions when it became greater than zero. For wild type EDL, an increase in muscle length caused small increases in baseline once the muscle was close to developing maximum force; this increase in baseline is associated with elongation of muscle elastic components. However, for many HyperKPP EDL, similar increases in baseline occurred very early in the maximization period when peak tetanic force was still very small (Fig. 3-2B and C). Sudden increases in baseline could also be observed between elicited contractions, some of very short duration as in Fig. 3-2B and

FIGURE 3-1

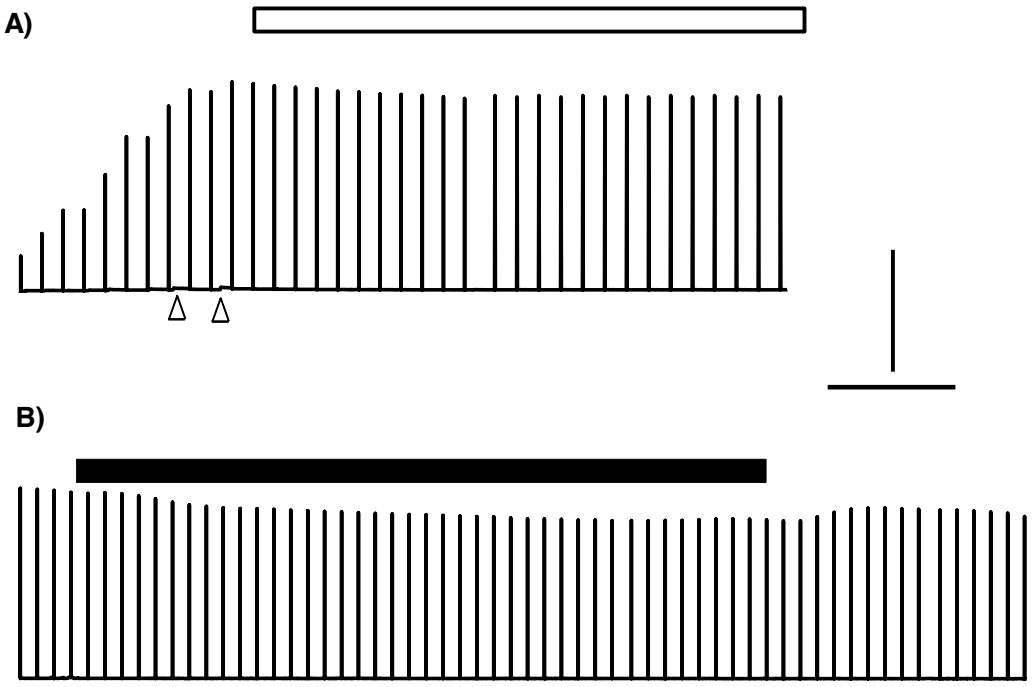

Figure 3-1. Representative recorder traces of the change in force for a wild type EDL muscle. The recorder trace was generated by acquiring and averaging three data points every 2 sec for the baseline; when a contraction was elicited, the minimum and maximum values were plotted. A) Changes in peak tetanic force during the period of muscle lengthening until maximum force is obtained followed by a 30 min equilibrium period. B) The decrease in peak tetanic force when $[K^+]_e$ is increased from 4.7 mM to 11 mM and the recovery of force when $[K^+]_e$ was returned to 4.7 mM. Symbols: open bar, equilibrium period; close bar, exposure to 11 mM K^+; vertical bar, 10 g; horizontal bar, 10 min.

FIGURE 3-2

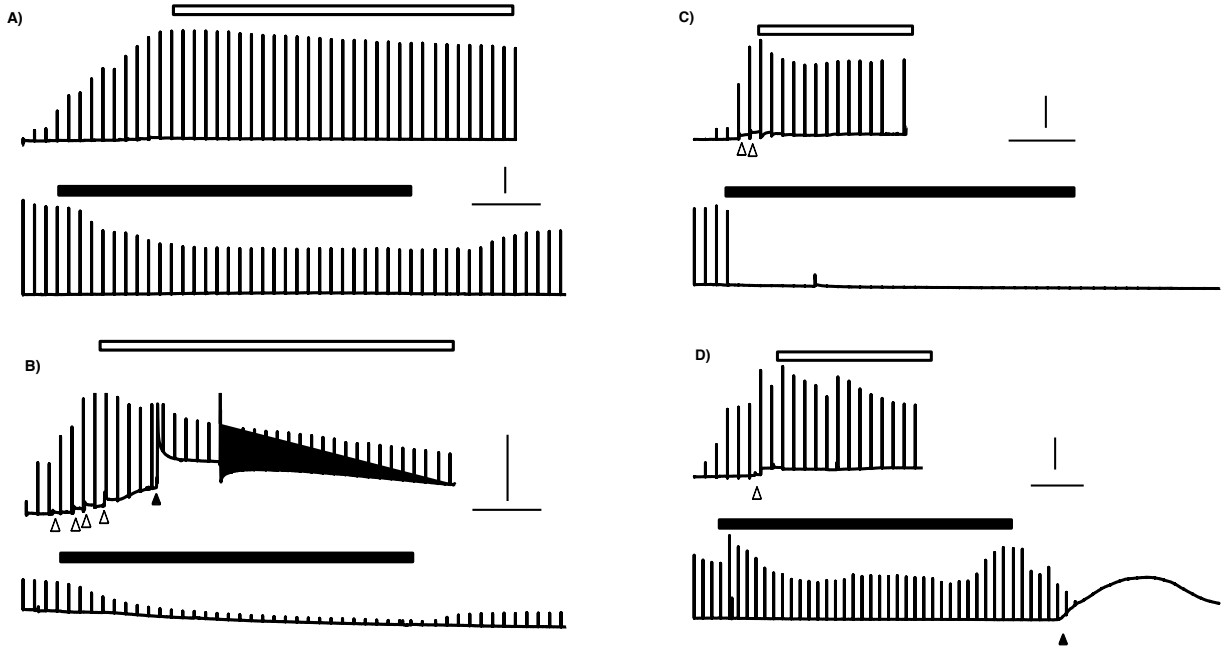

Figure 3-2. Recorder traces of tetanic force from HyperKPP EDL. The generation of the recorder trace and experimental protocol were as described in Fig. 3-1. A) One month, 2.4 mM $[Ca^{2+}]_e$; B) Four months, 1.3 mM $[Ca^{2+}]_e$; C) Four months, 1.3 mM $[Ca^{2+}]_e$; D) 12 months, 1.3 mM $[Ca^{2+}]_e$. For each group of traces, top trace is when the muscle was lengthened and the 30 min equilibrium period; bottom trace is the exposure to 11 mM K^+. Symbols: open bar, equilibrium period; close bar, exposure to 11 mM K^+; vertical bar, 5 g; horizontal bar, 10 min; Δ, small increase in baseline when muscles was stretched, ▲, sudden increase in baseline associated with a contracture; i.e., the increase in force was not elicited by an electrical contraction.

some of prolonged duration as in Fig. 3-2D. Associated with these sudden contractures were decreases in peak tetanic force elicited by electrical stimulation.

Complete and sudden loss of force were observed either following the increase in $[K^+]_e$ to 11 mM (Fig. 3-2C) or even during the maximization or equilibrium period for no apparent reason (data not shown).

TETANIC FORCE

EDL muscles

Once the tetanic force stopped increasing during the maximization period, a digitized contractile waveform was saved to analyze all parameters of the tetanic contraction. For wild type muscles, the peak tetanic force of that contraction represented the maximum tetanic force obtained during an experiment because these muscles constantly lost force over time, albeit at a very slow rate. However, for HyperKPP muscles, the maximum tetanic force was not always observed at that time because in a minority of cases peak tetanic force started to increase at one point during an experiment (data not shown). So, the peak tetanic force measured at the end of maximization was named the 'initial peak tetanic force.' For EDL of one-month-old wild type mice, the mean initial tetanic force was 30 N/cm^2 when exposed to 1.3 mM Ca^{2+} (Fig. 3-3A, inset). When the paired EDL was exposed to 2.4 mM Ca^{2+} mean initial force was 32 N/cm^2, representing a 5% difference. For HyperKPP EDL, the initial tetanic forces were significantly less when compared to wild type EDL, at both 1.3 and 2.4 mM Ca^{2+}, being only 13.3 and 15.8 N/cm^2 at 1.3 and 2.4 mM Ca^{2+}, respectively, representing an 18% difference.

After a 30-minute equilibrium period at 1.3 mM Ca^{2+}, peak tetanic force of wild type EDL was 28.8 N/cm^2, representing a 4 % decrease in force (Time 0 min in Fig. 3-3A). The

FIGURE 3-3

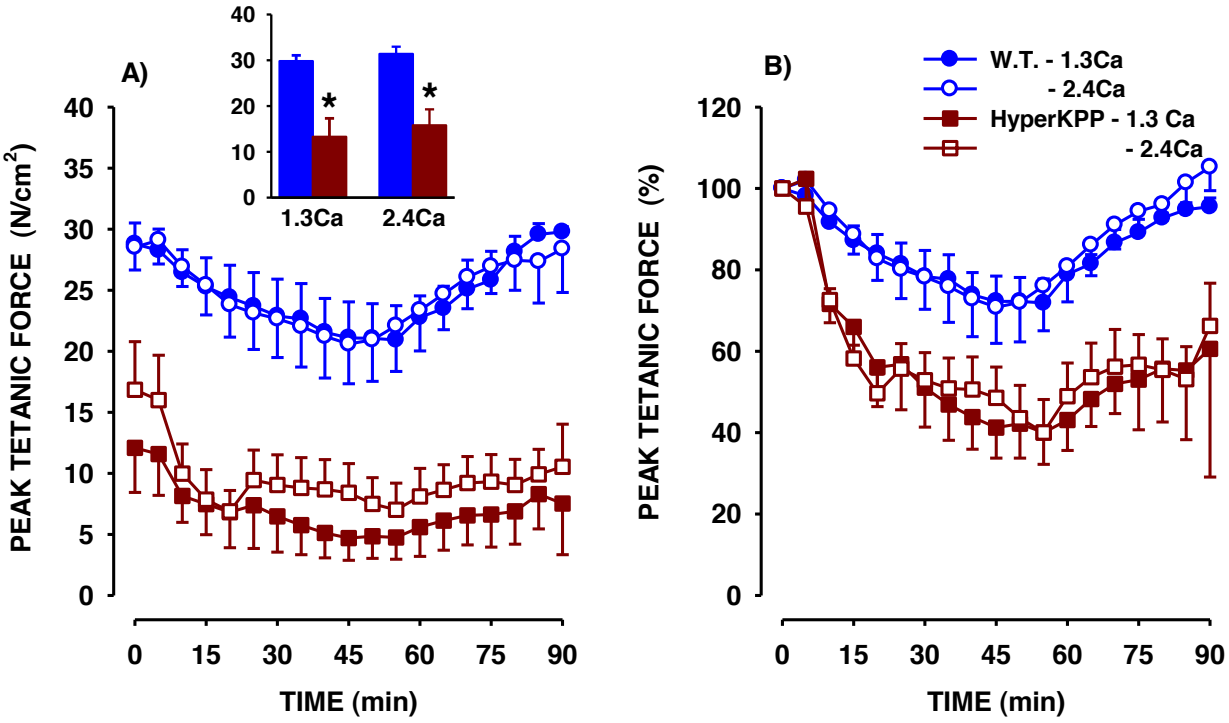

Figure 3-3. HyperKPP EDL muscles have lower peak tetanic force than wild type EDL. The effects of an increase in $[K^+]_e$ were tested while $[Ca^{2+}]_e$ was either 1.3 or 2.4 mm Ca^{2+}. EDL were obtained from one month old mice. A) Maximum tetanic force, which represents the maximum force developed by a muscle, was always measured at the beginning of an experiment. B) Changes in peak tetanic force when $[K^+]_e$ was increased from 4.7 (control) to 11 mM at time 0 min. Vertical bars are the S.E. of 5 muscles.

* Mean peak tetanic force was significantly less in HyperKPP than in wild type EDL, ANOVA and L.S.D. $P < 0.05$. (Not shown in B for clarity).

changes in peak tetanic force were quite similar for the wild type EDL exposed at 2.4 mM Ca^{2+}. A decrease in peak tetanic force during the equilibrium period was also observed for HyperKPP EDL at 1.3 mM from 13.3 to 12.1 N/cm^2; i.e. a 9% decrease. However, at 2.4 mM Ca^{2+}, mean peak tetanic force was 16.8 N/cm^2, representing an increase of 1 N/cm^2.

Studies on the effect of $[K^+]_e$ on force development usually report the changes in force using percent values. However, the variability of the data with HyperKPP muscles was such that changes in percent were actually not significant, even for decreases exceeding 50% (see example in Fig. 3-4C). So, for this study, peak tetanic forces are reported in both normalized values (i.e., in N/cm^2) and as a percent of the peak tetanic force under control conditions (i.e., 4.7 mM K^+), the latter to be used for comparisons with other studies. When $[K^+]_e$ was increased from 4.7 to 11 mM K^+, mean peak tetanic force of wild type EDL decreased in a similar fashion at 1.3 and 2.4 mM Ca^{2+} (Fig. 3-3A) from 28-29 to 22-23 N/cm^2 (Fig. 3-3A) or by 23-24% (Fig. 3-3B). For HyperKPP EDL, the decrease in mean peak tetanic force at 2.4 mM Ca^{2+} was initially greater than at 1.3 mM so that no differences were observed at 15 and 20 min. Thereafter, mean tetanic force continued to decrease at 1.3 mM Ca^{2+} while it slightly increased at 2.4 mM, so that at 55 minutes the mean peak tetanic forces were 5 and 7 N/cm^2 at 1.3 and 2.4 mM Ca^{2+}, respectively. On a relative scale, the decreases in force were not different between 1.3 and 2.4 mM Ca^{2+}, but were twice as large for HyperKPP compared to wild type EDL. Finally, when $[K^+]_e$ was returned to 4.7 mM K^+, mean peak tetanic forces of wild type EDL fully returned to the levels observed prior to the K^+ challenge, a recovery that was not observed with HyperKPP EDL.

Similar experiments were carried out with EDL muscles from mice that were 0.5, 1, 4 and 12 months old. Wild type EDL muscles from mice of different ages generated on average

mean peak tetanic force that were not significantly different, as previously described by Gong & Renaud (2003). So, the data were pooled together to simplify the presentation of the data. Mean initial tetanic force produced by EDL was significantly lower from young HyperKPP mice that were 0.5, 1 and 4 months old compared to that of wild type EDL (Fig. 3-4A). Mean tetanic forces at 1.3 mM Ca^{2+} were respectively 4.5, 12.8 and 8.1 N/cm^2. Although the force appeared highest at one month, one of the five HyperKPP EDL generated 24.6 N/cm^2. When that value was excluded, the average tetanic force became 9.9 N/cm^2 ± 2.8; i.e. similar to that of four-month-old HyperKPP EDL mice. So, most EDL from HyperKPP mice between the ages of 0.5 and four months generated less than one third of the force generated by wild type EDL. Interestingly, EDL from the 12-month HyperKPP mice produced a mean initial tetanic force that was not significantly different from that of the wild type EDL, albeit the initial tetanic forces ranged from 11.8 to 39.6 N/cm^2; i.e., some HyperKPP EDL still produced low tetanic force even at 12 months.

HyperKPP EDL from mice exposed to 2.4 mM Ca^{2+} (Fig. 3-4D) generated significantly higher initial tetanic force compared to those at 1.3 mM Ca^{2+}. Respectively, mean initial forces were 12.8, 15.8, and 18.2 N/cm^2 for two weeks, one, and four months old HyperKPP mice, which was 65, 16, 56 and 9% significantly higher than the initial force of HyperKPP EDL exposed to 1.3 mM $[Ca^{2+}]_e$.

Following an 11 mM K^+ challenge at 1.3 mM Ca^{2+}, wild type steady state tetanic force significantly decreased from 30 to 22 N/cm^2 (Fig. 3-4B). Peak tetanic forces at 11 mM K^+ were always less in HyperKPP than wild type EDL, even from 12-month-old HyperKPP mice (Figure 3-3B). Again, mean peak tetanic forces of HyperKPP EDL at 11 mM K^+ were higher at 2.4 mM than at 1.3 mM Ca^{2+}, but still significantly lower than wild type (Fig 3-4E).

At 1.3 mM Ca^{2+}, the percent decreases in peak tetanic force appeared greater in HyperKPP than wild type EDL, except from mice that are 0.5 months old (Fig. 3-4C). A similar situation was observed at 2.4 mM Ca^{2+} with one anomalous case (Fig. 3-4F). The mean percent tetanic force of four month old EDL was 128% because one of the five tested EDL had an initial force 0.9 N/cm^2 that increased suddenly to 4.2 N/cm^2 ten minutes into the K^+ challenge, giving rise to a 367% increase in force. When this value is omitted, then the mean peak tetanic force at 11 m K^+ was just 54.6 ±. 14.6 N/cm^2, a value closer to those observed at one and 12 months. Finally, while the extent of percent decreases in tetanic force observed in this study are always significant in other studies, the ANOVA for the percent changes in this study indicated no significant difference between mice of different ages because of the large variability among HyperKPP muscles.

Soleus

Similar to EDL, soleus muscles were gradually lengthened with increasing stimulation to reach maximum tetanic force (Fig. 3-5A). The responses of HyperKPP soleus during an experiment were also quite variable between muscles with unstable baseline (Fig. 3-8); such variable responses were not observed with wild type soleus (data not shown). As observed for HyperKPP EDL, some soleus muscles had relatively stable tetanic force, baseline and small decreases in tetanic force during the K^+ challenge (Fig. 3-5A), which for these muscles constituted an increased in $[K^+]_e$ from 4.7 to 10 mM because wild type soleus is more sensitive to K^+ than wild type EDL (Cairns et al., 1997). For other soleus, peak tetanic force gradually increased during maximization as observed in wild type muscles, but then began losing force during the equilibrium period (Fig. 3-5B). In this case, the K^+ challenge was started before the full 30-minute equilibrium was completed. During the K^+

FIGURE 3-4

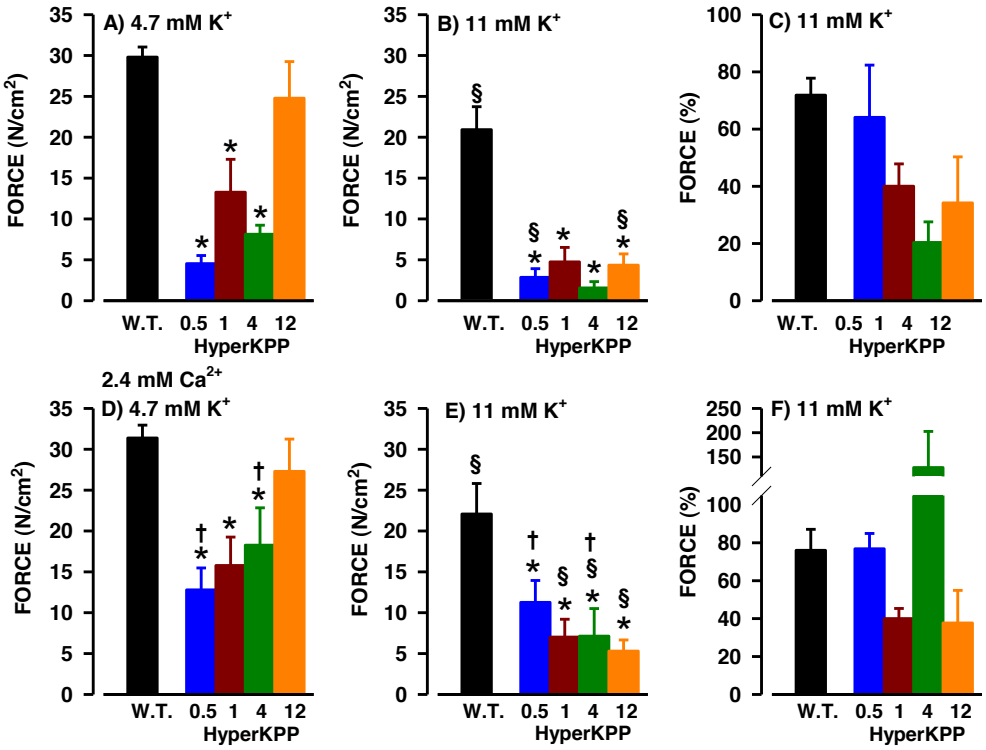

Figure 3-4. Peak tetanic force is significantly lower in HyperKPP EDL than wild type muscles. EDL were tested at either 1.3 (A-C) or 2.4 (D-F) mM Ca^{2+}. A, D) Maximum peak tetanic force measured at the start of each experiment at 4.7 mM K^+. B, E) Peak tetanic force after 55 min at 11 mM K^+. C, F) Peak tetanic force after 55 min at 11 mM K^+ but expressed as a percent of the tetanic force at 4.7 mM K^+. Vertical bars represent the S.E. of 4-5 muscles.

* Peak tetanic force of HyperKPP EDL significantly different from that of wild type EDL.

§ Peak tetanic force at 11 mM K^+ significantly different from that at 4.7 mM K^+.

† Peak tetanic force at 1.3 mM Ca^{2+} significantly different from that at 2.4 mM Ca^{2+}.

challenge the baseline became unstable or increased with very large force loss.

Figure 3-5C shows an example of a HyperKPP soleus that generated low maximum tetanic force and was very unstable during the maximization period. Spontaneous increases and decreases in baseline were clearly observed with a short period during which electrical stimulations failed to generate a contraction. Upon exposure to 10 mM K^+, peak tetanic force decreased very rapidly with an increase in baseline. Contrary to the situation in Fig. 3-5B, a return of $[K^+]_e$ to 4.7 mM allowed for force recovery, which ended up being higher than prior to the K^+ challenge. Figure 3-5D shows an example where the increase in force during the maximization period appeared normal, but then during the equilibrium period there was a sudden loss in the capacity to contract. After a contracture, the capacity to generate tetanic force resumed followed by large decreases in force at 10 mM K^+ with no recovery upon a return to 4.7 mM K^+.

On an average basis, the mean initial peak tetanic force of wild type soleus at 1.3 mM Ca^{2+} was 24.1 N/cm^2 (Fig. 3-6A). Soleus from HyperKPP mice between 0.5 to 12 months of age generated less force than those from wild type mice; however, significant differences were observed only at 0.5 months old mice. The mean initial peak tetanic forces generated by HyperKPP soleus at 1.3 mM Ca^{2+} were 4.9, 16.3, 18.2 and 18.1 N/cm^2 for two weeks, one, four and twelve months, respectively. Except for soleus from HyperKPP 0.5 months old mice, HyperKPP soleus was affected to a lesser extent than HyperKPP EDL for all age groups tested. That is, the differences in initial peak tetanic force between wild type and HyperKPP muscles at 1.3 mM Ca^{2+} were smaller for soleus than for EDL. Furthermore, there was significantly less variability in peak tetanic force amongst muscles within a given age group compared to that of the HyperKPP EDL. For example, for one-month-old mice, the range of

FIGURE 3-5

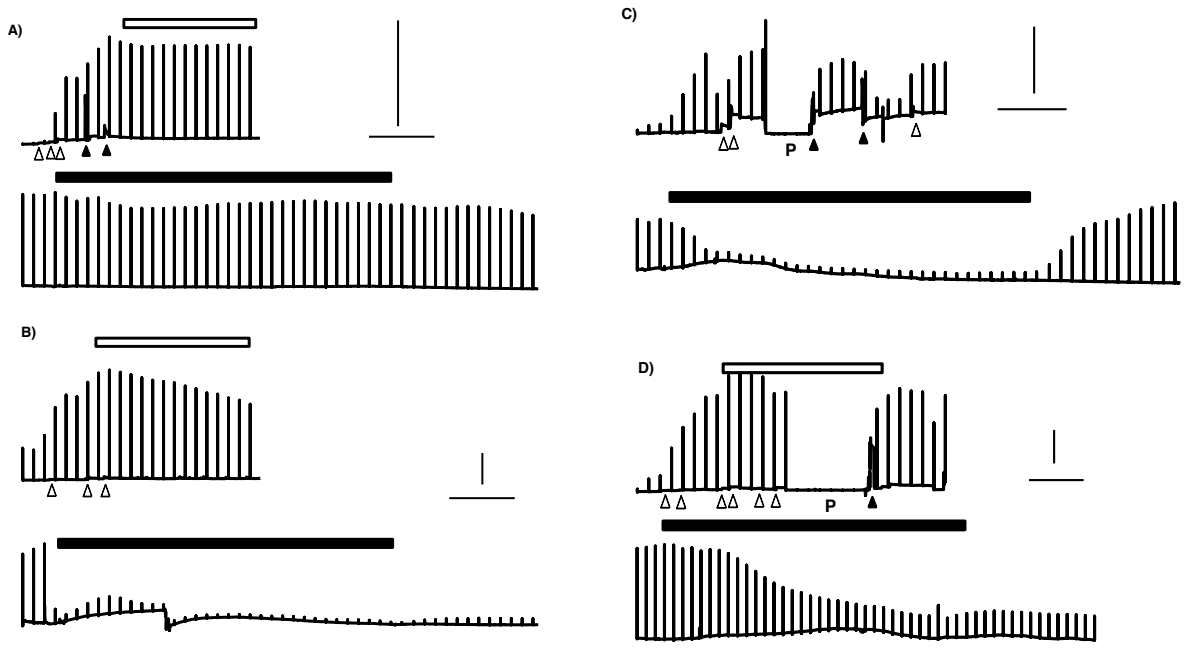

Figure 3-5. Recorder traces of tetanic force from HyperKPP soleus. The generation of the recorder trace and experimental protocol were as described in Fig. 3-1. A) one month, 1.3 mM $[Ca^{2+}]_e$; B) 12 months, 1.3 mM $[Ca^{2+}]_e$; C) 4 months, 1.3 mM $[Ca^{2+}]_e$; D) 4 months, 1.3 mM $[Ca^{2+}]_e$. For each group of traces, top trace is when the muscle was lengthened and the 30 min equilibrium period; bottom trace is the exposure to 10 mM K^+. Symbols: open bar, equilibrium period; close bar, exposure to 11 mM K^+; vertical bar, 5 g; horizontal bar, 10 min; Δ, small increase in baseline when muscles was stretched, ▲, sudden increase in baseline associated with a contracture; i.e., the increase in force was not elicited by an electrical contraction; 'P' marked a period of complete loss of tetanic force; i.e., no force development during electric stimulation possibly due to paralysis.

initial peak tetanic forces generated by HyperKPP soleus was 14.1 to 17.7 N/cm^2, whereas for HyperKPP EDL it was from 1.58 to 24.63 N/cm^2. Mean initial peak tetanic forces for HyperKPP soleus muscles at 2.4 mM Ca^{2+} (Fig. 3-6D) were higher than those at 1.3 mM Ca^{2+}. However, significant differences were only observed at one and four months, being 23 and 29% higher at 2.4 mM Ca^{2+}, respectively.

Following a 10 mM K^+ challenge at 1.3 mM Ca^{2+}, mean peak tetanic forces of wild type soleus significantly decreased by 7.33 N/cm^2 (Fig. 3-6B), representing a 33% decrease (Fig. 3-6B, C). Mean peak tetanic forces at 10 mM K^+ were always less in HyperKPP than wild type soleus by at least 50%, even from 12-month-old HyperKPP mice (Figure 3-6B). The percent decreases in peak tetanic force were also greater for HyperKPP than wild type soleus (Fig. 3-6C). As for the EDL, one anomalous situation was again observed for the data at 0.5 months.

Here, the initial force of one HyperKPP soleus was 0.9 N/cm^2 and increased to 4.9 N/cm^2 while exposed to 10 mM K^+, resulting in a 444% increase in force. Another HyperKPP soleus had an initial tetanic force of 9.5 N/cm^2, increasing eventually to 10.8 N/cm^2, giving rise to a 14% increase. So, again while the differences are highly significant on an absolute scale, they were not significant on a relative scale. Mean peak tetanic force of HyperKPP soleus at 2.4 mM Ca^{2+} were significantly greater than at 1.3 mM Ca^{2+} only at one month, while they were mostly significantly lower than those of wild type soleus (Fig. 3-6E). Once again, the percent decreases in force at 10 mM K^+ were greater for HyperKPP than wild type soleus (except at 0.5 months) but significant differences were not observed due to the large variability.

FIGURE 3-6

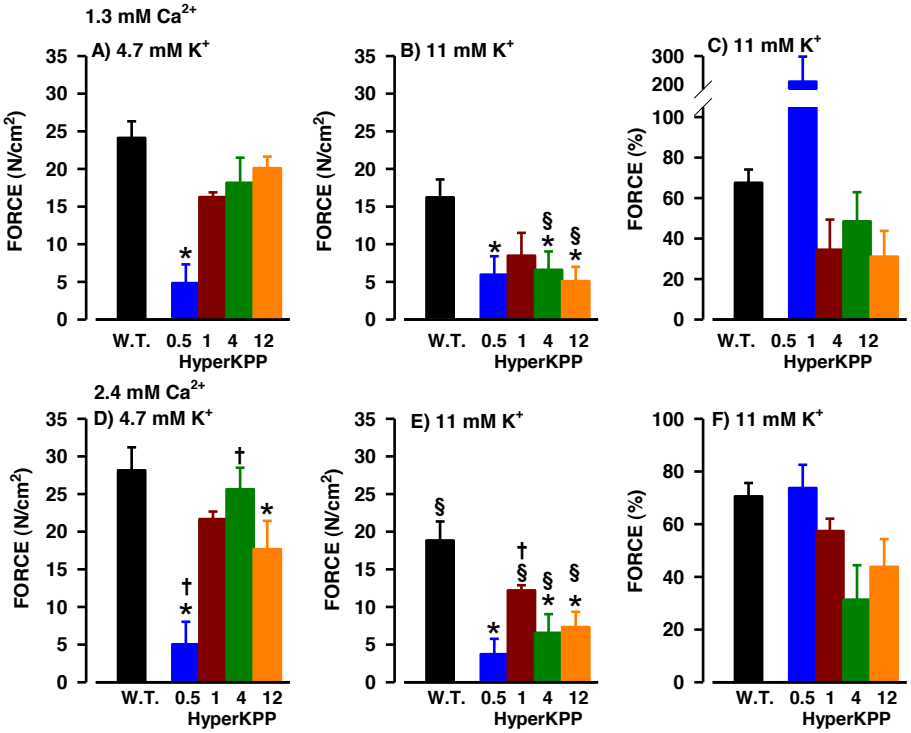

Figure 3-6. Peak tetanic force is significantly lower in HyperKPP soleus than wild type soleus. Soleus were tested at either 1.3 (A-C) or 2.4 (D-F) mM Ca^{2+}. A, D) Maximum peak tetanic force measured at the start of each experiment at 4.7 mM K^+. B, E) Peak tetanic force after 55 min at 11 mM K^+. C, F) Peak tetanic force after 55 min at 11 mM K^+ but expressed as a percent of the tetanic force at 4.7 mM K^+. Vertical bars represent the S.E. of 4-5 muscles.

* Peak tetanic force of HyperKPP soleus significantly different from that of wild type soleus.

§ Peak tetanic force at 11 mM K^+ significantly different from that at 4.7 mM K^+.

† Peak tetanic force at 1.3 mM Ca^{2+} significantly different from that at 2.4 mM Ca^{2+}.

UNSTIMULATED FORCE

One major feature of the contractile behavior of HyperKPP EDL and soleus is the unstable and sometimes large increases in baseline (Fig. 3-2, 3-5). The increases in baseline are most likely due to some contractures following the generation of uncontrolled action potentials. The force being generated during these contractures are different from the tetanic force, which are generated when contractions are elicited by electrical stimulation. Unstimulated force was therefore defined as the force generated by those contractures. For this study, the maximum unstimulated force is reported, defined as the highest unstimulated force observed during an experiment, either during maximization, equilibrium or the K^+ challenge. Wild type EDL and soleus did not produce any unstimulated force (data as shown in Fig. 3-1). For HyperKPP EDL, the average maximum unstimulated force was 0.54, 1.27, 2.30, and 1.67 N/cm^2 for two weeks, one, four and twelve months old mice, respectively (Fig. 3-7A). However, the amount of unstimulated force amongst HyperKPP EDL was highly variable. For example, unstimulated force for the four-month age group ranged from 0.11 to 5.31 N/cm^2. More importantly, when these unstimulated forces are compared to the mean peak tetanic force of wild type EDL, it was found that out of a total of 20 tested HyperKPP EDL, seven generated unstimulated force that was equivalent or more than 5% of the mean peak tetanic force of wild type EDL, with three of them being over 10%. HyperKPP EDL generated less unstimulated force at 2.4 mM Ca^{2+} (Fig. 3-7B).

In general, HyperKPP soleus generated more unstimulated force (Fig. 3-8) than HyperKPP EDL with mean values ranging between 2.13 and 4.52 N/cm^2. Those means were equivalent to more than 10% of the mean peak tetanic force of wild type soleus. Furthermore, for three muscles the unstimulated force was more than 20% of the tetanic

FIGURE 3-7

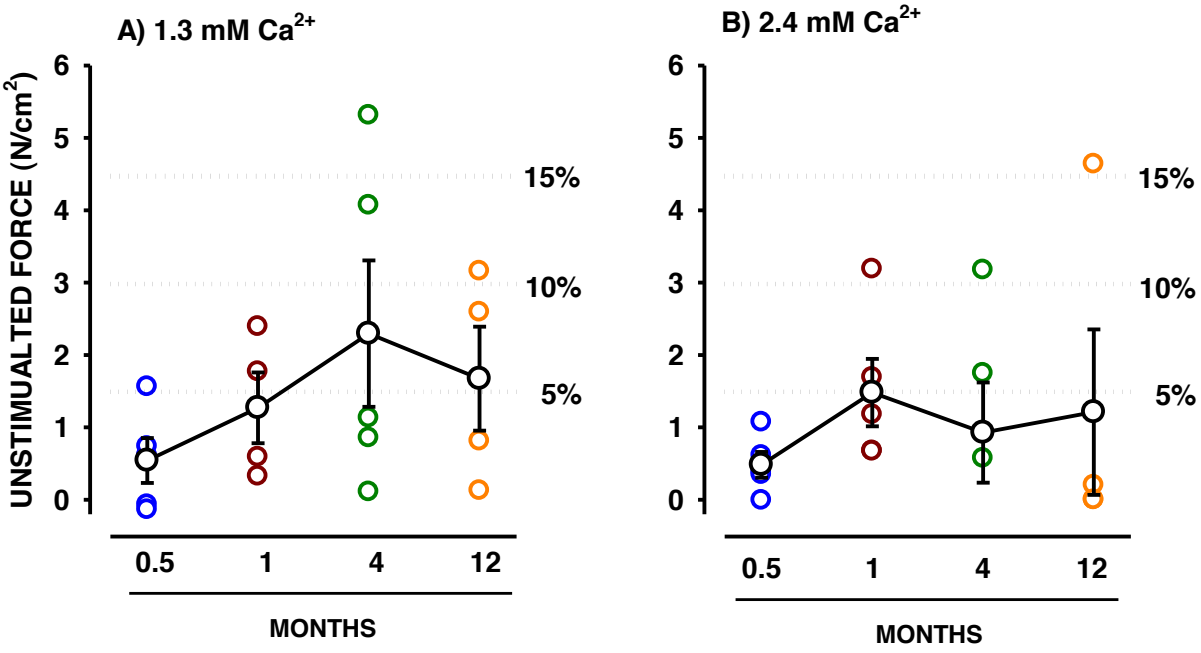

Figure 3-7. HyperKPP EDL developed large amount of unstimulated force. Unstimulated force reported here represents the maximum force observed during an experiment. Wild type EDL did not generate any unstimulated force (data not shown). Dashed lines represent the amount of force relative to the mean peak tetanic force observed in wild type EDL. Mean unstimulated force for each time period is shown by symbols linked by lines. Vertical bars represent the S.E. of 4-5 muscles.

FIGURE 3-8

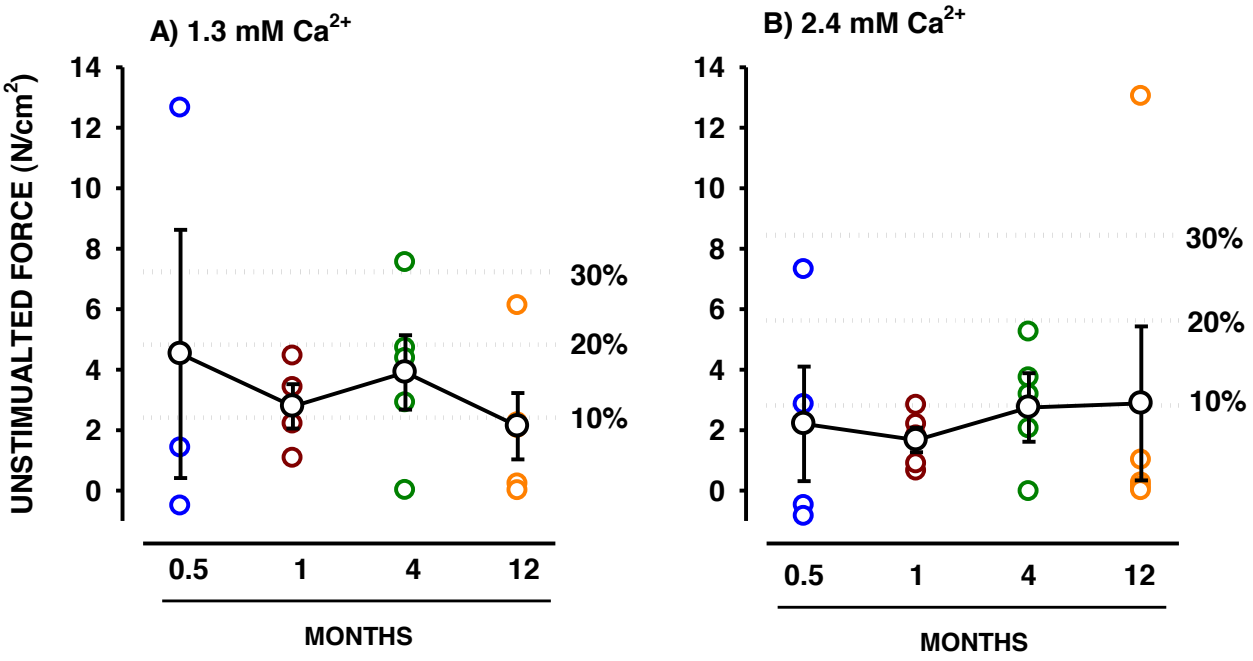

Figure 3-8. HyperKPP soleus developed large amount of unstimulated force. Unstimulated force reported here represents the maximum force observed during an experiment. Wild type soleus did not generate any unstimulated force (data not shown). Dashed lines represent the amount of force relative to the mean peak tetanic force observed in wild type soleus. Mean unstimulated force for each time period is shown by symbols linked by lines. Vertical bars represent the S.E. of 4-5 muscles.

force generated by wild type soleus. On an average basis, the mean unstimulated force of HyperKPP soleus was less at 2.4 than 1.3 mM Ca^{2+}, but the difference was not significant.

TIME KINETICS

On an average basis, half-rise time and half–relaxation time of HyperKPP EDL and soleus were not significantly different from those observed from wild type EDL (Table 1).

EXPERIMENTAL TEMPERATURE

Tetanic force

In this study, the experimental temperature was 37°C because it is physiologically relevant. However, results from EDL and soleus are different from those of Hayward et al. (2008) and Clausen et al. (2011, see Discussion for further details). One possible reason for the differences is because their studies were carried at 25°C and 30°C, respectively. So, some experiments were carried out to determine how K^+ effects on muscle contractility are modulated by temperature. For one set of experiments wild type soleus was used because it is more stable over time than EDL. At 37°C, an increase in $[K^+]_e$ from 4.7 to 10 mM caused a decrease in mean peak tetanic force from 25.4 to 9.1 N/cm^2, representing a 52% decrease (Fig. 3-9). The initial tetanic forces at 25°C were smaller, being on average 18.0 N/cm^2. During the K^+ challenge, tetanic force decreased to 4.4 N/cm^2, representing a 73% decrease in peak tetanic force. Interestingly, an increase in experimental temperature from 25° to 37°C while soleus were at 10 mM K^+ allowed for an increased in tetanic force toward the force observed in soleus kept at 37°C throughout the experiments. Thus, on a relative scale, the K^+ effects were much greater at 25° than at 37°C.

PARAMETERS	MUSCLE	MOUSE	AGE (months)	1.3 mM Ca^{2+}	2.4 mM Ca^{2+}
½-Rise Time	EDL	W.T.		17.8 ± 1.0 (4)	18.6 ± 3.2 (5)
(ms)		HyperKPP	0.5	23.8 ± 0.8 (5)*	21.0 ± 1.1 (5)
			1.0	18.6 ± 1.7 (5)	20.2 ± 0.9 (5)
			4.0	18.0 ± 1.8 (5)	21.7 ± 2.4 (5)
			12.0	16.9 ± 1.7 (5)	15.6 ± 0.9 (4)
½-Relaxation Time		W.T.		24.9 ± 5.4 (4)	38.1 ± 9.3 (5)
(ms)		HyperKPP	0.5	31.1 ± 2.7 (5)	34.2 ± 3.6 (5)
			1.0	22.2 ± 1.9 (5)	22.3 ± 1.2 (5)
			4.0	30.2 ± 8.5 (5)	49.4 ± 9.1 (5)
			12.0	23.9 ± 2.2 (5)	24.0 ± 1.6 (4)
½-Rise Time	SOLEUS	W.T.		43.2 ± 2.2 (5)	41.6 ± 1.6 (5)
(ms)		HyperKPP	0.5	40.0 ± 8.4 (3)	43.5 ± 1.5 (2)
			1.0	40.4 ± 1.0 (5)	42.1 ± 2.8 (5)
			4.0	43.7 ± 5.0 (5)	37.5 ± 2.5 (4)
			12.0	39.9 ± 2.0 (5)	41.9 ± 2.0 (5)
½-Relaxation Time		W.T.		67.5 ± 14.2 (5)	68.4 ± 13.8 (5)
(ms)		HyperKPP	0.5	103.1 ± 56.1 (3)	70.7 ± 0.1 (2)
			1.0	53.2 ± 5.4 (5)	69.6 ± 6.8 (5)
			4.0	45.4 ± 10.0 (5)	65.8 ± 10.7 (4)
			12.0	51.3 ± 6.6 (5)	60.8 ± 4.3 (5)

Table 3. Half-rise time and half-relaxation time for wild type and HyperKPP EDL and soleus muscles. For wild type muscles, the data from different ages were pooled together.

* Significantly different from wild type value, ANOVA and L.S.D. $P < 0.05$.

The behavior of EDL muscles was then tested at 25° and 37°C for both wild type and HyperKPP mice. The EDL was used to document the temperature effect since this muscle was more affected by the disease. Using paired muscles, one was tested at 25°C and the other at 37°C. Wild type EDL muscles generated significantly more peak tetanic force at 37°C as the mean force was 30.7 N/cm^2 compared to 23.3 N/cm^2 at 25°C (Fig. 3-10A). However, the same was not observed for HyperKPP EDL. Mean peak tetanic force in HyperKPP EDL muscles was actually significantly lower at 37°C then at 25°C, generating 8 N/cm^2 and 14 N/cm^2, respectively. As previously mentioned, muscles slowly lose force over time. For wild type EDL, the mean force lost during the 30-minute equilibrium period was 5.5-5.8% at both temperatures (Fig. 3-10B). The loss was much higher and significant at 37°C, being respectively 16.7% and 38.4% at 25° and 37°C.

Muscles were then exposed to a 10 mM K^+ challenge for 60 minutes as per the study of Hayward et al. (2008). The mean tetanic force of wild-type EDL muscles at 25°C decreased from 23.3 to 15.2 N/cm^2 in 60 min, representing a 35% decrease (Fig. 3-10C, E). At 37°C, tetanic force decreased from 30.7 to 19.6 N/cm^2, representing a 30% decrease, which was quite similar to that at 25°C. The tetanic force of HyperKPP EDL muscles at 25°C decreased by about 33%, which was comparable to the wild type EDL at the same temperature (Fig. 3-10D,F). However, the decrease in force at 10 mM K^+ was significantly greater at 37°C, being 53%. Furthermore, a return to 4.7 mM K^+ allowed the force of wild type EDL to return to normal at both temperatures and for HyperKPP EDL at 25°C only. It thus appears that HyperKPP EDL muscles are more sensitive to the K^+ challenge at 37° than at 25°C.

FIGURE 3-9

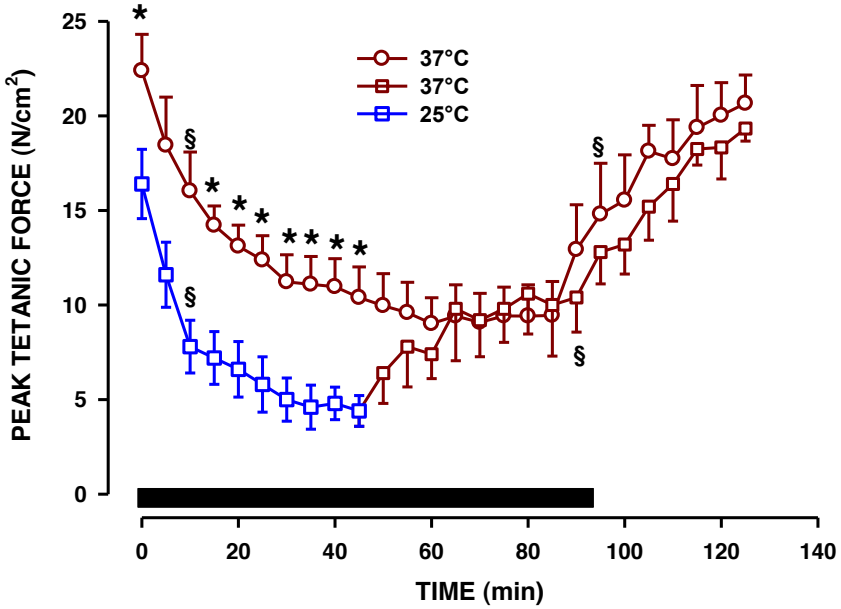

Figure 3-9. Wild type soleus muscles have less peak tetanic force at 25°C than at 37°C. The effects of an increase in $[K^+]e$ were tested while $[Ca^{2+}]e$ was 2.4 Ca^{2+} and temperature was either 25 ºC or 37 ºC. Once muscles at 25° reached steady state, temperature was increased to 37°. Soleus muscles were obtained from two-month-old mice.

§ Indicate when the first and last peak tetanic forces that were significantly different from the force at Time 0 min

* Peak tetanic force at 37°C significantly different from the force at 25°C.

ANOVA $P<0.05$

FIGURE 3-10

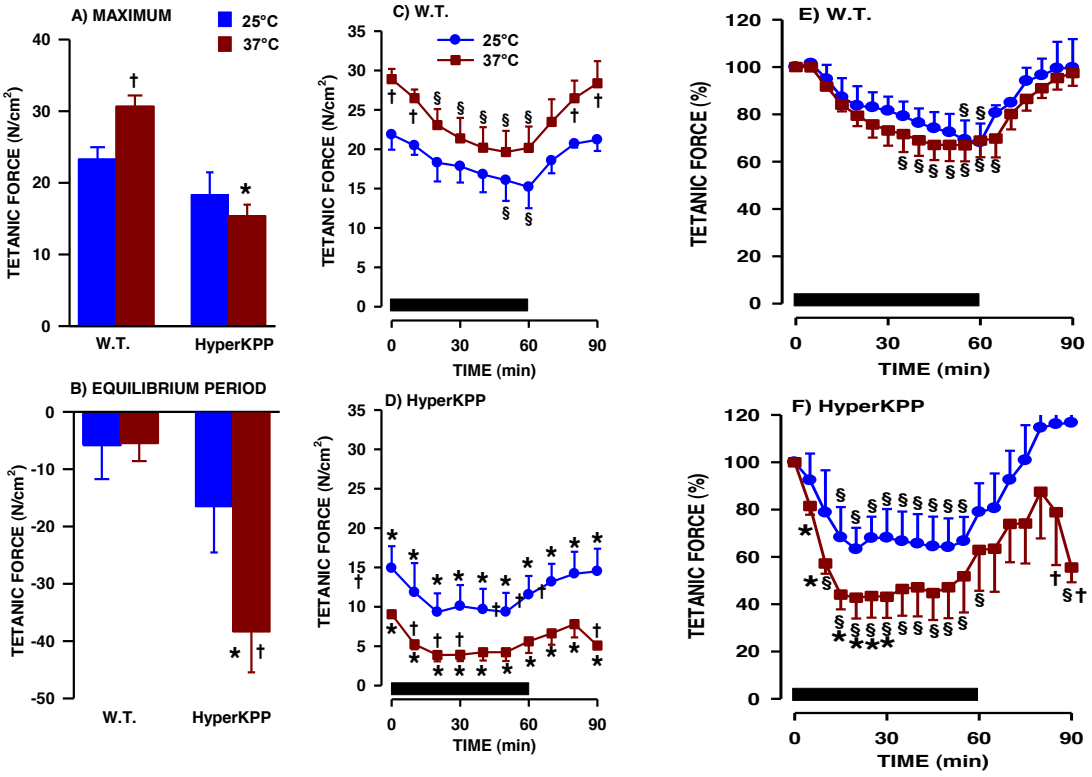

Figure 3-10. HyperKPP EDL muscles have much less peak tetanic force at 37°C than at 25°C. The effects of an increase in $[K^+]e$ were tested while $[Ca^{2+}]e$ was 1.3 Ca^{2+} and temperature was either 25 ºC or 37 ºC. EDL were obtained from two month old mice. A) Initial peak tetanic force, which represents the maximum force developed by a muscle, was always measured at the beginning of an experiment. B) Changes in tetanic force during the 30-minute equilibrium period. C and D) Changes in absolute peak tetanic force at 25 ºC and 37 ºC when $[K^+]e$ was increased from 4.7 (control) to 10 mM K^+ at time 0 min in F) wild-type and D) HyperKPP. E and F) Changes in relative peak tetanic force at 25 ºC and 37 ºC when $[K^+]e$ was increased from 4.7 (control) to 10 mM K^+ at time 0 min in E) wild-type and F) HyperKPP. Vertical bars are the S.E. of 5 muscles.

Mean peak tetanic force was significantly less in HyperKPP than in wild type EDL, ANOVA and L.S.D. $P < 0.05$. (Not shown in B for clarity).

* Significantly different from the tetanic force of wild type EDL.

§ Significantly different from the tetanic force at Time 0 min

† Significantly different from the tetanic force at 25°C.

ANOVA $P<0.05$

Unstimulated force

Wild type EDL had very little unstimulated force at 25° and 37°C, and all of it was actually the tension from the elastic components as muscles were being stretched (Fig. 3-11A). At 25°C, HyperKPP EDL had similar unstimulated force when compared to wild type EDL muscles. At 37°C, however, large and significantly greater unstimulated force were observed, being 3.4-fold greater than at 25°C and being equivalent to 8.7% of the mean peak tetanic force of wild type EDL at 37°C. In these experiments, unstimulated force decreased during the 10 mM K^+ challenge, except for a small increase for the wild type EDL at 37°C (Fig. 3-11B, C).

CALCIUM

It has been previously shown that administration of calcium gluconate helps to relieve the symptoms of HyperKPP attacks. Hayward et al. (2008) tested the Ca^{2+} effect, but only during recovery from the K^+ challenge. Here, experiments were performed using paired muscles while $[Ca^{2+}]_e$ was 1.3 mM during the dissection, maximization and equilibrium period and the other at 4.0 mM Ca^{2+}. It has been previously shown that skeletal muscle exposed to high $[Ca^{2+}]$ at 37°C will generate an increased peak tetanic force (Godt & Lindley, 1982). As expected, wild type EDL muscles generated greater peak tetanic force at higher $[Ca^{2+}]_e$, generating a mean tetanic force of 25.2 and 34.8 N/cm^2 at 1.3 and 4.0 mM Ca^{2+}, respectively (Fig. 3-12A). In this series of experiments, all HyperKPP EDL failed to contract at 1.3 mM Ca^{2+} while generating a mean initial of less than 1 N/cm^2. After the equilibrium period, the $[Ca^{2+}]_e$ was switched. There was no significant change in steady-state tetanic force of wild type EDL when $[Ca^{2+}]_e$ was increased from 1.3 to 4.0 mM Ca^{2+}; however, steady-state tetanic force decreased in the paired muscles when $[Ca^{2+}]_e$ was decreased from

4.0 to 1.3 mM Ca^{2+} by 36% over a 90 minute period (Fig. 3-12B). The same was observed for HyperKPP EDL when $[Ca^{2+}]_e$ was reduced to 1.3 mM Ca^{2+}, but an increase in $[Ca^{2+}]_e$ from 1.3 to 4.0 mM did not result in an increased tetanic force (Fig. 3-12C).

FIGURE 3-11

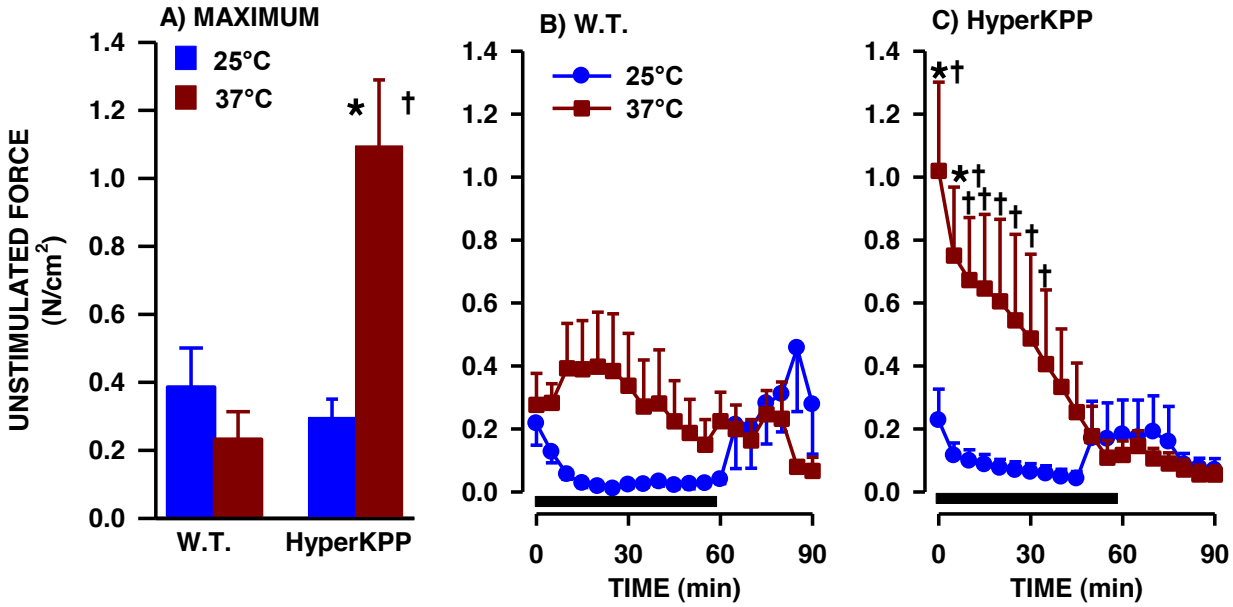

Figure 3-11. HyperKPP EDL muscles at 37°C have greater unstimulated force than at 25°C. The effects of unstimulated force were measured from the beginning of the experiment and calculated based on the changes in baseline from the beginning of the experiment. A) Maximum unstimulated force measured at the start of each experiment at 4.7 mM K^+ at 25 and 37°C. B) Changes in unstimulated force in wild type EDL when $[K^+]_e$ was increased from 4.7 (control) to 10 mM at time 0 min at 25 and 37°. C) Changes in unstimulated force in HyperKPP EDL when $[K^+]_e$ was increased from 4.7 (control) to 10 mM at time 0 min at 25 and 37°C. Vertical bars are the S.E. of 5 muscles.

* Significantly different from wild type EDL.

† Significantly different from 25°C.

ANOVA, $P < 0.05$

FIGURE 3-12

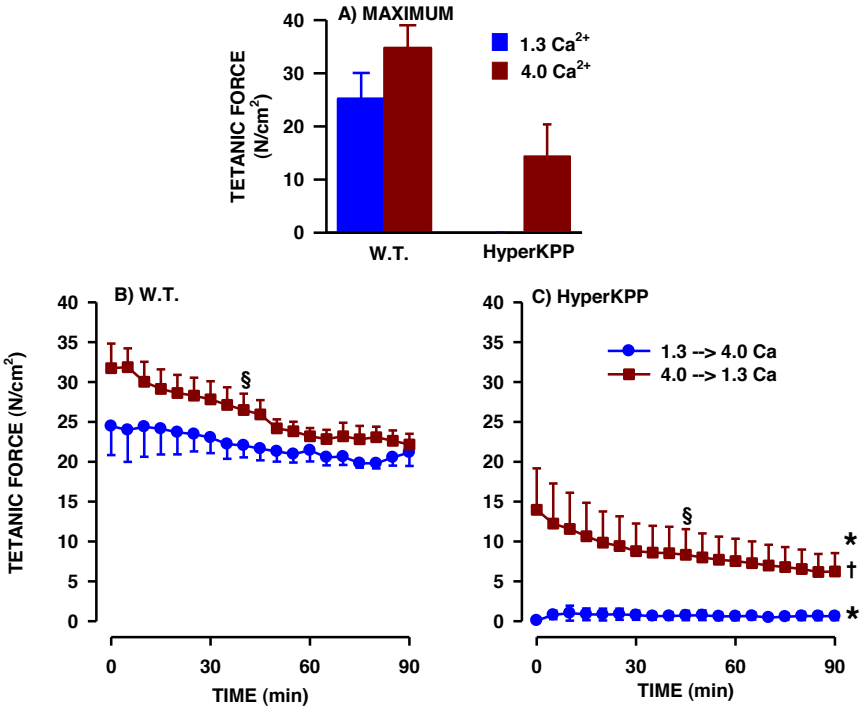

Figure 3-12. Changes in the contractile response of HyperKPP EDL is greater at 1.3 mM Ca^{2+} than 4.0 mM Ca^{2+}. EDL were obtained from two-month-old mice. A)Maximum peak tetanic force measured at the start of an experiment while $[Ca^{2+}]_e$ was either 1.3 or 4.0 mM. B) Steady state peak tetanic force at either 1.3 mM Ca^{2+} or 4.0 mM Ca^{2+} in wild type EDL. C) Steady state peak tetanic force at either 1.3 mM Ca^{2+} or 4.0 mM Ca^{2+} in HyperKPP EDL.

§ Indicate when tetanic force became significantly different from Time 0 min

* Indicate that all tetanic forces are significantly different from those of wild type EDL for each time period

† Indicate that all tetanic forces significantly different from those at 1.3 mM Ca^{2+}.

ANOVA, $P < 0.05$

CHAPTER 5

DISCUSSION

The major findings of the study are: i) as previously reported at 25°C and 30°C (Clausen et al., 2011; Hayward et al., 2008) the initial peak tetanic force of HyperKPP EDL and soleus at 37°C were lower and the K^+ effect is greater in HyperKPP muscles than those of wild type muscles; ii) however, the differences in initial forces between wild type and HyperKPP and the K^+ effect were the largest at 37°C; iii) the effects of the disease on force were greater in EDL than soleus; iv) there was more unstimulated force in HyperKPP muscles at 37°C; v) HyperKPP soleus generated more unstimulated force than EDL; vi) there was no difference in ½-rise or-½ relaxation between wild type and HyperKPP muscles; vii) there was greater force depression at 1.3 than 2.4 mM Ca^{2+} and viii) *in vitro*, the defect of muscle instability appeared as early as two weeks of age.

EXPERIMENTAL MODEL AND APPROACHES

The M1592V mouse model

Two previous studies (Clausen et al., 2011; Hayward et al., 2008), this study and some ongoing studies (Renaud laboratory, unpublished results) have demonstrated that the HyperKPP mouse model, generated by a knock in of the equivalent human M1592V mutation in the mouse genome, exhibits several distinctive features of the disease in humans. These features include: i) myotonic activity and paralysis *in vivo*; ii) greater Na^+ influx in resting muscle; iii) greater sensitivity to the K^+-induced for depression; iv) alleviation of weakness with increased [Ca^{2+}] *in vitro*; v) development of non-episodic muscle weakness with aging; vi) increase in muscle fiber damage; vii) increase in oxidative capacity and viii) fiber type switching to a more oxidative phenotype. So, the knock in of the equivalent human

M1592V mutation in the mouse genome provides a way to study how HyperKPP affects the contractility of fast- and slow-twitch fibers. The use of EDL and soleus muscles also provides a model to study the mechanism of HyperKPP, at least for that mutation.

$[K^+]$

Individuals with HyperKPP have venous $[K^+]$ that ranges between 5 and 8 mM during a paralytic attack. During exercise, however, muscle interstitial $[K^+]$ exceeds plasma levels by 4-5 mM (Juel et al., 2000). It is therefore more than likely that myotonic discharges raise interstitial $[K^+]$ between 10-13 mM. Furthermore, considering the small size of the t-tubules, it is expected that t-tubular $[K^+]$ may even be higher. Hayward et al. (2008) have shown that increasing $[K^+]_e$ to 8 mM produced only transient weakness while 10 mM produced prolonged weakness in HyperKPP EDL tested at 25°C. For this study, $[K^+]_e$ of 10-11 mM were chosen because of their small effects on EDL and soleus tetanic force. However, considering that at those $[K^+]_e$, tetanic force was close to zero, further supports the notion that during a paralytic attack, the interstitial $[K^+]_e$ is close to or above 10-11 mM.

Temperature

In resting mouse, the subcutaneous and muscle temperature is close to 30-32°C (Burton et al., 1998). During exercise, however, the core body temperature of the rat increases 3-4°C, while the temperature of the skin, which does not generate heat but receives warm blood from active muscles, increases from 30°C to 36°C (Fuller et al., 1998; Gonzales-Alonso et al., 1999). Since the increase in body temperature is due to an increased heat production by muscles, it is then more likely that during exercise the temperature of muscles reaches or exceeds 37°C; and the same is expected during myotonic discharges.

Many investigators use experimental temperatures as low as 25°C in an attempt to

prevent a hypoxic/hypoglycemic core that develops when large size EDL and soleus muscles have hindered oxygen and glucose diffusion to the muscle core. When such conditions occur, the contractile characteristics are altered (Zhang et al., 2006). Studies at 37°C have become more feasible if the flow of physiological solution is maintained high as in this study; i.e. 15 ml/min. So, this is the first study on HyperKPP muscles carried out at 37°C, being the most physiological condition. The importance of the choice of experimental temperature is further illustrated by the fact that the steady-state voltage dependence of slow inactivation shifts in a depolarizing direction with increased temperature (Ruff, 1999) and the major cause of HyperKPP is a defect in slow inactivation.

The first two studies on mouse HyperKPP muscles were carried out at 25° and 30°C (Hayward et al., 2008; Clausen et al., 2011). Compared to this study, it appears that the effects of HyperKPP EDL force show smaller changes at 25°C than at 37°C. Also, at 30°C the HyperKPP effects were greater in soleus than in EDL, while the reverse was observed at 37°C. These differences may be related to differences in experimental temperatures. Tetanic force of rat soleus is more sensitive to elevated $[K^+]_e$ at 25°C than 37°C (Nielsen et al., 2003). However, Cairns et al. (2003) using mouse soleus, showed the opposite effect. So, a series of experiments were carried out to determine differences in K^+ effects at different temperatures for both wild type and HyperKPP muscles.

In wild type soleus, an increase in $[K^+]$ from 4.7 mM to 10 mM at 25°C causes faster and greater decreases in tetanic force than at 37°C. Furthermore, when the temperature was increased from 25°C to 37°C while maintaining $[K^+]_e$ at 10 mM, peak tetanic force increased to that at 37°C. So, these results agree with those of Nielsen et al. (2003) but not with Cairns et al. (2003). In Cairns' setup, muscles were positioned in a vertical chamber and the

physiological solution was constantly bubbled, resulting in very small fluid movement near muscles compared to our fast flow above and below. Thus, there might be better muscle oxygenation in the setup of this study than in Cairns' setup, and the apparent greater effect of K^+ at 37°C may be due to the development of an anoxic core over time that further reduces force. It is therefore suggested that wild type muscles, at least the soleus, is more sensitive to the K^+-induced force depression at 37°C than at lower temperatures.

Hayward et al. (2008) reported that at 25°C the initial peak tetanic force of HyperKPP EDL was 34% less than the wild type EDL force. Figure 3-4 shows a difference of 61% at 37°C. When paired HyperKPP EDL muscles were tested at 25° and 37°C, the differences were respectively 21% and 50%. So, despite the variability of the contractile responses of HyperKPP muscles, a hallmark feature of the disease, the data suggest that the symptoms are worse at 37°C. This study also demonstrated that at 37°C, HyperKPP muscles are more unstable, as they lose more tetanic force over time and generated large amount of unstimulated force.

HyperKPP EDL vs. soleus

In this study, differences between wild type and HyperKPP soleus muscles were much smaller than those for EDL. One possible explanation is that $Na_{v1.4}$ protein content is four-times less in soleus than EDL. Furthermore, Na^+ influx, at least during action potentials, are 5-6 times less than in EDL (Clausen et al., 2004). However, recent studies have demonstrated that TTX-sensitive Na^+ influx in resting muscle were as large in HyperKPP soleus as EDL, with both being much higher than their respective wild type muscles (Barbalinardo & Renaud, unpublished results). So, for now it remains unclear as to why soleus is less sensitive than EDL at 37°C.

As mentioned above, the differences between HyperKPP EDL and soleus are the reverse of those observed by Clausen et al. (2011), who reported that the HyperKPP soleus was affected to a greater extent than EDL. However, they carried out their study at 30°C and used a stimulation of muscles at 120 Hz, while in this study the stimulation frequencies were 200 and 140 Hz for EDL and soleus, respectively. Perhaps, the HyperKPP effects are not only temperature dependent, but they may also be frequency dependent.

Ca^{2+} EFFECTS

Calcium gluconate is known to alleviate HyperKPP symptoms. In their study, Hayward et al. (2008) demonstrated an improved recovery of force following a K^+ challenge when $[Ca^{2+}]_e$ was increased from 1.3 to 4 mM. This study is the first to demonstrate that it also improve contractility from three points of view. First, it improved the initial peak tetanic force of both EDL and soleus muscle. Second, it reduced the extent of the K^+-induced force depression. For the latter, the effects were not always significant, which is in agreement with the fact that calcium treatment is not fully effective for HyperKPP patients. Third, exposing HyperKPP muscles to 1.3 mM often caused full loss of tetanic force, an effect not observed at higher $[Ca^{2+}]_e$.

The mechanism by which Ca^{2+} modulates recovery of tetanic force in HyperKPP muscle is unknown. In wild type muscles, Ca^{2+} hyperpolarizes the resting membrane potential and restores force in the presence of elevated $[K^+]_e$. It is thus possible that Ca^{2+} also reduces the depolarization at high $[K^+]_e$. This possibility is further supported by the fact that reducing $[Ca^{2+}]_e$ from 4.0 to 1.3 mM caused similar decrease in peak tetanic force in wild type and HyperKPP EDL.

AGING

HyperKPP is a complex disease in terms of: i) unpredictability of symptom occurrence between and within patients even with the same mutation; ii) onset of symptoms starting between six months and ten years of age and iii) worsening of symptoms until adolescence.. A major objective for this M.Sc. thesis was therefore to follow how the disease progresses, focusing on the apparition of symptoms by measuring contractile defects of EDL and soleus between the ages of two weeks and twelve months in relation to the $Na_{v1.4}$ content in muscles.

This study now reports that HyperKPP EDL is most affected both in terms of initial force and decrease at 11 mM K^+ between two weeks and four months of age, with some improvement in initial peak tetanic force at 12 months of age. For HyperKPP soleus, a defective contractile response in terms of initial force was very large at two weeks, followed by some improvements between the ages of one and twelve months, while decreased force at 10 mM K^+ was defective at all ages. Periods of paralytic attacks were also observed in HyperKPP mice. These attacks were observed when mice were on their side or when they were dragging themselves with their forelimbs, with the hind limbs dragging behind (data not shown). More importantly, these attacks were observed in mice as young as three weeks of age (they could not easily be observed prior to that time as they were with their mother). Thus, the contractile defects appeared to have an onset by two-three weeks of age.

In mouse, $Na_{v1.4}$ protein content reaches its maximum by the age of three weeks (Zhou & Hoffman, 1994). The same situation has recently been confirmed for HyperKPP muscles (Ammar & Renaud, unpublished results). Furthermore, there are no significant differences in tetrodotoxin-dependent Na^+ influx in HyperKPP muscles between 0.5, two and

four months of age (Barbalinardo & Renaud, unpublished results). Thus, contractile defects are clearly observed before the $Na_{v1.4}$ content and defective Na^+ influx reaches its maximum in the cell membrane, with no sign of symptoms worsening thereafter. It is therefore suggested that all HyperKPP symptoms are all dependent on defective $Na_{v1.4}$ channels and do not depend on subsequent changes in gene expression, which actually appear to start by the age of one and a half months and are completed by the age of two months, at least in EDL (Khogali & Renaud, unpublished results).

So, as previously proposed, evidence of myotonic discharge is likely due to persistent Na^+-influx through non-inactivating defective Na^+ channels, causing depolarization to the membrane, thus generating uncontrolled AP's. As $[K^+]_e$ increases due to the K^+ efflux with AP repolarization, there are excessive membrane depolarizations that eventually inactivate too many Na_v channels, rendering the membrane completely unexcitable and thus resulting in paralysis.

CONCLUSION

The onset of symptoms in HyperKPP mice occurs at a time when $Na_{v1.4}$ protein content reaches its maximum in life. No evidence was obtained for a worsening of symptoms after the channel has reached its maximum content. Thus, this study supports the hypothesis that all HyperKPP symptoms are related to the defective $Na_{v1.4}$ channel, making this disease different from its counterpart, HypoKPP, for which mutations are on $Ca_{v1.1}$ or $Na_{v1.4}$, but the paralysis also involves defective $K_{ir2.1}$ and $K_{ir6.2}$ channels.

REFERENCE LIST

Adams JA, Dwyer TM, & Hille B (1980). The permeability of endplate channels to monovalent and divalent metal cations. *Journal of General Physiology* 75, 493-510.

Adrian RH & Bryant SH (1974). On the repetitive discharge in myotonic muscle fibers. *J Physiol (Lond)* 240, 505-515.

Ambrose C, Cheng S, Fontaine B, Nadeau JHMM, & Gusella JF (1992). The alpha-subunit of the skeletal muscle sodium channel is encoded proximal to Tk-1 on mouse chromosome 11. *Mamm Genome* 3, 151-155.

Amin A, Asghari-Roodsari A, & Tan HL (2010). Cardiac sodium channelopathies. *Pflugers Arch* 450, 223-237.

Armstrong CM, Bezanilla F, & Rojas E (1973). Destruction of sodium conductance inactivation in squid axons perfused with pronase. *Journal of General Physiology* 62, 375-391.

Armstrong CM, Bezanilla F, & Rojas E (1977). Inactivation of the sodium channel II. Gating current experiments. *Journal of General Physiology* 70, 567-590.

Ashcroft FM & Gribble FM (1998). Correlating structure and function in ATP-sensitive K^+ channels. *Trends in Neuroscience* 21, 288-294.

Bendahhou S, Cummins TR, Kula RW, Fu YH, & Ptácek LJ (2002). Impairment of slow inactivation as a common mechanism for periodic paralysis in DIIS4-S5. *Neurology* 58, 1266-1272.

Bennett AL, Ware FJ, Dunn AL, & McIntyre AR (1953). The normal membrane resting

potential of mammalian skeletal muscle measured *in vivo*. *J Comp Physiol* 42, 343-375.

Bennett ES (2001). Channel cytoplasmic loops alter voltage-dependent sodium channel activation in an isoform-specific manner. *J Physiol (Lond)* 535, 371-381.

Boyden PA & Jeck CD (1995). Ion channel function in disease. *Cardiovasc Res* 29, 312-318.

Boyle PJ & Conway EJ (1941). Potassium accumulation in muscle and associated changes. *J Physiol (Lond)* 100, 1-63.

Bradley WG, Taylor R, Rice DR, Hausmanowa-Petruzewicz I, Adelman LS, Jenkison M, Jedrzejowska H, Drac H, & Pendlebury WW (1990). Progressive myopathy in hyperkalemic periodic paralysis. *Arch Neurol* 47, 1013-1017.

Brinkmeier H, Zachar E, & Rüdel R (1991). Voltage-dependent K^+ channels in the sarcolemma of mouse skeletal muscle. *Pflugers Arch* 419, 486-491.

Brooks GA, Hittelman KJ, & Faulkner JA (1971). Tissue temperatures and whole-animal oxygen consumption after oxygen. *Am J Physiol* 221, 427-431.

Brooks JE (1969). Hyperkalemic periodic paralysis. Intracellular electromyographic studies. *Arch Neurol* 20, 13.

Brooks SV & Faulkner JA (1988). Contractile properties of skeletal muscles from young, adult and aged mice. *J Physiol (Lond)* 404, 71-82.

Bruton JD, Lännergren J, & Westerblad H (1998). Effects of CO_2-induced acidification on the fatigue resistance of single mouse muscle fibers at 28°C. *J Appl Physiol* 85, 478-483.

Buchthal F, Engbaek L, & Gamstrop I (1958a). Paresis and hyperexcitability in Adynamia episodica hereditaria. *Neurology* 8, 347-351.

Buchthal F, Engbaek L, & Gamstrop I (1958b). Some aspects of the pathophysiology of Adynamia episodica hereditaria. *Dan Med Bull* 5, 167-169.

Cairns SP, Buller SJ, Loiselle DS, & Renaud JM (2003). Changes of action potentials and force at lowered $[Na^+]_o$ in mouse skeletal muscle: implication for fatigue. *Am J Physiol Cell Physiol* 285, C1131-C1141.

Cairns SP, Flatman JA, & Clausen T (1995). Relation between extracellular $[K^+]$, membrane potential and contraction in rat soleus muscle: modulation by the Na^+-K^+ pump. *Pflugers Arch* 430, 909-915.

Cairns SP, Hing WA, Slack JR, Mills RG, & Loiselle DS (1997). Different effects of raised $[K^+]_o$ on membrane potential and contraction in mouse fast- and slow-twitch muscle. *Am J Physiol* 273, C598-C611.

Cannon SC (2000). Spectrum of sodium channel disturbances in the nondystrophic myotonias and periodic paralyses. *Kidney International* 57, 772-779.

Cannon SC (2006). Pathomechanisms in channelopathies of skeletal muscle and brain. *Annu Rev Neurosci* 29, 387-415.

Cannon SC, Brown RH, & Corey DP (1991). A sodium channel defect in hyperkalemic periodic paralysis: Potassium-induced failure of inactivation. *Neuron* 6, 691-626.

Cannon SC, Brown RH, & Corey DP (1993). Theorical reconstruction of myotonia and paralysis caused by incomplete inactivation of sodium channels. *Biophys J* 65, 270-288.

Cannon SC, Hayward LJ, Beech J, & Brown RH (1995). Sodium channel inactivation is impaired in equine hyperkalemic periodic paralysis. *Journal of Neurophysiology* 73, 1892-1899.

Catterall WA (1992). Cellular and molecular biology of voltage-gated sodium channels. *Physiol Rev* 72S, S15-S48.

Catterall WA (1995). Structure and function of voltage-gated ion channels. *Annual Review of*

Biochemistry 64, 493-531.

Celesia GG (2001). Disorders of membrane channels or channelopathies. *Clinical Neurophysiology* 112, 141-164.

Chahine M, Bennett PB, George Jr. AL, & Horn R (1994). Functional expression and properties of the human skeletal muscle sodium channel. *Pflugers Arch* 427, 136-142.

Cifelli C, Bourassa F, Gariépy L, Banas K, Benkhalti M, & Renaud JM (2007). K_{ATP} channel deficiency in mouse FDB causes fiber damage and impairs Ca^{2+} release and force development during fatigue in vitro . *J Physiol (Lond)* 582, 843-857.

Clausen T & Everts ME (1991). K^+-Induced inhibition of contractile force in rat skeletal muscle: Role of active Na^+-K^+ transport. *Am J Physiol Cell Physiol* 261, C799-C807.

Clausen T & Nielsen OB (1994). The Na^+,K^+-pump and muscle contractility. *Acta Physiol Scand* 152, 365-373.

Clausen T, Nielsen OB, Clausen JD, Pedersen T, & Hayward LJ (2011). Na^+, K^+-pump stimulation improves contractility in isolated muscles of mice with hyperkalemic periodic paralysis. *Journal of General Physiology* 138, 117-130.

Clausen T, Wang PH, Orskov H, & Kristensen O (1980). Hyperkalemic periodic paralysis: Relationships between changes in plasma water, electrolytes, insulin and catecholamines during attacks. *Scand J Clin Lab Invest* 40, 211-220.

Creutzfeldt OD, Abbott BC, Fowler WM, & Pearson CM (1963). Muscle membrane potentials in episodic adynamia. *Electrocephal Cli Neurophysiol* 15, 508-519.

Cummins TR & Sigworth FJ (1996). Impaired slow inactivation in mutant sodium channels. *Biophys J* 71, 227-236.

Cummins TR, Zhou J, Sigworth FJ, Ukomadu C, Stephan M, Ptácek LJ, & Agnew WS

(1993). Functional consequences of a Na^+ channel mutation causing hyperkalemic periodic paralysis. *Neuron* 10, 667-678.

De Luca A, Mambrini M, & Camerino DC (1990). Changes in membrane ionic conductances and excitability characteristics of rat skeletal muscle during aging. *Pflugers Arch* 415, 642-644.

de Silva SM, Kunci R, Griffin JW, Cornblath DR, & Chavoustile S (1990). Paramyotonia congenita or hyperkalemic periodic paralysis? Clinical and electrophysiological features of each entity in one family. *Muscle Nerve* 13, 21-26.

Doupnik CA, Davidson N, & Lester HA (1995). The inward rectifier potassium channel family. *Curr Op NeuroBiol* 5, 268-277.

Dulhunty AF (1979). Distribution of potassium and chloride permeability over the surface and t-tubule membranes of mammalian skeletal muscle. *J Membr Biol* 45, 293-310.

Ebers GC, George AL, Barchi RL, Ting-Passador SS, Kallen RG, Lathrop GM, Beckmann JS, Hahn AF, Brown WF, Campbell RN, & Hudson AJ (1991). Paramyotonia congenita and hyperkalemic periodic paralysis are linked to the adult muscle sodium channel gene. *Ann Neurol* 30, 810-816.

Fahlke C, Beck CL, & George Jr. AL (1997). A mutation in autosomal dominant myotonia congenita affects pore properties of the muscle chloride channel. *Proc Natl Acad Sci* 94, 2729-2734.

Fakler B, Brandle U, Glowatzki E, Weidmann S, Zenner HP, & Ruppersberg JP (1995). Strong voltage-dependent inward rectification of inward rectifier K^+ channels is caused by intracellular spermine. *Cell* 80, 149-154.

Fenn WO (1937). Loss of potassium in voluntary contraction. *Am J Physiol* 120, 675-680.

Fenn WO (1938). Factors affecting the loss of potassium from stimulated muscles. *Am J Physiol* 124, 213-227.

Filatov GN & Rich MM (2004). Hyperpolarized shifts in the voltage dependence of fast inactivation of $Na_{V1.4}$ and $Na_{V1.5}$ in rat model of critical illness myopathy. *J Physiol (Lond)* 559, 813-820.

Fontaine B, Khurana TS, Hoffman EP, Bruns GAP, Haines JL, Trofatter JA, Hanson MP, Rich J, McFarlane H, Yasek DM, Romano D, Gusella JF, & Brown RH (1990). Hyperkalemic periodic paralysis and the adult muscle sodium channel α-subunit gene. *Science* 250, 1000-1002.

Fraser JA, Christopher L, Huang H, & Pedersen T (2011). Relationships between resting conductances, excitability, and t-system ionic homeostasis in skeletal muscle. *Journal of General Physiology* 138, 95-116.

Fuller A, Carter RN, & Mitchell D (1998). Brain and abdominal temperatures at fatigue in rats exercising in the heat. *J Appl Physiol* 84, 877-883.

Gamstrop I, Hauge M, Helweg-Larsen HF, Mjönes H, & Sagild U (1957). Adynamia episodica hereditaria. A disease clinically resembling familial periodic paralysis but characterized by increasing serum potassium during the paralytic attacks. *Am J Med* 23, 385-390.

George Jr. AL, Komisarof J, Schwartz LS, Nicholas H, & Hoffman EP (1992). Primary structure of the adult human skeletal muscle voltage-dependent sodium channel. *Ann Neurol* 31, 131-137.

Godt RE & Lindley BD (1982). Influence of temperature upon contractile activation and isometric force production in mechanically skinned muscle fibers of the frog. *J Gen Physiol*

80, 279-297.

Goldin AL, Barchi RL, Caldwell JH, Hofmann F, Howe JR, Hunter JC, Kallen RG, Mandel G, Meisler MR, Netter YB, Noda M, Tamkun MM, Waxman SG, Wood JN, & Catterall WA (2000). Nomenclature of voltage-gated sodium channel. *Neuron* 28, 365-368.

Gong B, Legault D, Miki T, Seino S, & Renaud JM (2003). K_{ATP} channels depress force by reducing action potential amplitude in mouse EDL and soleus. *Am J Physiol Cell Physiol* 285, C1464-C1474.

Gonzales-Alonso J, Teller C, Andersen SL, Jensen FB, Hyldig T, & Nielsen B (1999). Influence of body temperature on the development of fatigue during prolonged exercise in the heat. *J Appl Physiol* 86, 1032-1039.

Hanna WJB, Tsushima RG, Sah R, McCutcheon LJ, Marban E, & Backx PH (1996). The equine periodic paralysis Na^+ channel mutation alters molecular transitions between the open and inactivated states. *J Physiol (Lond)* 497, 349-364.

Harvey J & Zierler KL (1958). The production of very high extracellular potassium concentration in the intact rat and its effect on muscle membrane potential. *Physiologist* 1, 35.

Hayward LJ, Brown RH, & Cannon SC (1997). Inactivation defects caused by myotonia-associated mutations in the sodium channel III-IV linker. *J Gen Physiol* 107, 559-576.

Hayward LJ, Kim JS, Lee M-Y, Zhou H, Kim.J.W., Misra K, Salajegheh M, Wu F-F, Matsuda C, Reid V, Cros D, Hoffman EP, Renaud JM, Cannon SC, & Brown RH (2008). Targeted mutation of mouse $Na_{V1.4}$ muscle sodium channel produces myotonia and potassium-sensitive weakness. *J Clin Invest* 118, 1437-1449.

Hayward LJ, Sandoval GM, & Cannon SC (1999). Defective slow inactivation of sodium channels contribute to familial periodic paralysis. *Neurology* 52, 1447-1453.

Hodgkin AL & Horowicz P (1959). The influence of potassium and chloride ions on the membrane potential of single muscle fibres. *J Physiol (Lond)* 148, 127-160.

Hodgkin AL & Katz B (1949). The effect of sodium ions on the electrical activity of the giant axon of the squid. *J Physiol (Lond)* 108, 37-77.

Ji S, Sun W, George AL, Horn R, & Barchi RL (1994). Voltage-dependent regulation of modal gating in the rat SkM1 sodium channel expressed in *Xenopus* oocytes. *Journal of General Physiology* 104, 625-643.

Juel C, Pilegaard H, Nielsen JJ, & Bangsbo J (2000). Interstitial K^+ in human skeletal muscle during and after dynamic graded exercise determined by microdialysis. *Am J Physiol* 278, R400-R406.

Jurkat-Rott K & Lehmann-Horn F (2007). Genotype-Phenotype correlation and therapeutic rationale in hyperkalemic peridoic paralysis. *Neurotherapeutics* 4, 216-224.

Jurkat-Rott K, Lehmann-Horn F, Elbaz A, Heine R, Gregg RG, Hogan K, Powers PA, Laple P, Vale-Santos JE, Weissenback J, & Fontaine B (1994). Calcium channel mutation causes hypokalemic periodic paralysis. *Human Molecular Genetics* 3, 1415-1419.

Jurkat-Rott K, Mitrovic N, Hang C, Kouzmekine A, Iaizzo P, Herzog J, Lerche H, Nicole S, & Lehmann-Horn F (2000). Voltage-sensor sodium channel mutations cause hypokalemic periodic paralysis type 2 by enhanced inactivation and reduced current. *Proc Natl Acad Sci* 97, 11673.

Kallen RG, Sheng Z, Yang J, Chen L, Rogart RB, & Barchi RL (1990). Primary structure and expression of a sodium channel characteristic of denervated and immature rat skeletal muscle. *Neuron* 4, 233-242.

Kang SY, Kim J-S, Choi JC, Kang J-H, & Lee JS (2008). An unusual pathologic feature and

phenotype associated with familial hyperkalemic periodic paralysis. *European Journal of Neurology* 15, e47-e48.

Kelly P, Rime CS, Recan D, Millasseau P, Eymard B, Pelletier J, Thomas C, Chapon F, & Desnuelle C (1997). Paramyotonia congenita and hyperkalemic periodic paralysis associated with a Met 1592 Val substitution in the skeletal muscle sodium channel alpha subunit- a large kindred with a novel phenotype. *Neuromuscular Dis* 7, 105-111.

Klein R, Egan T, & Usher P (1960). Changes in sodium, potassium and water in hyperkalemic familial periodic paralysis. *Metabolism* 9, 1005-1025.

Kontis KJ, Rounaghi A, & Goldin AL (1997). Sodium channel activation gating is affected by substitutions of voltage sensor positive charges in all four domains. *Journal of General Physiology* 110, 391-401.

Kraner SD, Tanaka JC, & Barchi RL (1985). Purification and functional reconstitution of the voltage-sensitive sodium channel from rabbit T-tubular membranes. *J Biol Chem* 260, 6341-6347.

Kraner SD, Yang J, & Barchi RL (1989). Structural inferences for the native skeletal muscle sodium channel as derived from patterns of endogenous proteolysis. *J Biol Chem* 264, 13273-13280.

Kubo Y, Baldwin TJ, Jan YN, & Jan LY (1993). Primary structure and functional expression of a mouse inward rectifier potassium channel. *Nature* 362, 127-133.

Kubota T, Kinoshita M, Sasaki R, Aoike F, Takahashi M, Sakoda S, & Hirose K (2009). New mutation of the Na channel in the severe form of potassium-aggravated myotonia. *Muscle Nerve* 39, 666-673.

Kyle DJ & Ilyin V (2007). Sodium channel blockers. *Journal of medicinal chemistry* 50,

2583-2588.

Layzer RB (1967). Hyperkalemic periodic paralysis. *Arch Neurol* 16, 455.

Lehmann-Horn F & Jurkat-Rott K (1999). Voltage-gated ion channels and hereditary disease. *Physiol Rev* 79, 1317-1372.

Lehmann-Horn F, Küther G, Ricker K, Grafe P, Ballanyi K, & Rüdel R (2007a). Adynamia episodica hereditaria with myotonia: a non-inactivating sodium current and the effect of extracellular pH. *Muscle Nerve* 10, 363-374.

Lehmann-Horn F, Rüdel R, Ricker K, Lorkovic H, Dengler R, & Hopf HC (2007b). Two cases of adynamia episodica hereditaria: in vitro investigation of muscle cell membrane and contraction parameters. *Muscle Nerve* 6, 113-121.

Li RA, Ennis IL, Tomaselli GF, & Marban E (2002). Structural basis of differences in isoform-specific gating and lidocaine block between cardiac and skeletal muscle sodium channels. *Mol Pharmacol* 61, 136-141.

Lindinger MI, Hawke TJ, Vickery L, Bradford L, & Lipskie SL (2001). An integrative, in situ approach to examining K^+ flux in resting skeletal muscle. *Can J Physiol Pharmacol* 79, 996-1006.

Lupa MT, Krzemien DM, Schaller KL, & Caldwell JH (1993). Aggregation of sodium channels during development and maturation of the neuromuscular junction. *J Neurosci* 13, 1326-1336.

Makita N, Bennett PB, & George AL (1994). Voltage-gated Na^+ channel B1 subunit mRNA expressed in adult human skeletal muscle, heart and brain is encoded by a single gene. *J Biol Chem* 269, 7571-7578.

Marban E (1998). Structure and function of voltage-gated sodium channels. *J Physiol (Lond)*

208, 647-658.

Matar W, Nosek TM, Wong D, & Renaud JM (2000). Pinacidil suppresses contractility and preserves energy but glibenclamide has no effect during fatigue in skeletal muscle. *Am J Physiol* 278, C404-C416.

Matthews E, Fialho D, Tan SV, Venance SL, Cannon SC, Sternberg D, Fontaine B, Amato AA, Barohn RJ, Griggs RC, & Hanna.M.G. (2009). The non-dystrophic myotonias: molecular pathogenesis, diagnosis and treatment. *Brain*.

McArdle B (1962). Adynamia episodica hereditaria and its treatment. *Brain* 85, 121-148.

Medbo JI & Sejersted OM (1990). Plasma potassium changes with high intensity exercise. *J Physiol (Lond)* 421, 105-122.

Messner DJ & Catterall WA (1985). The sodium channel from rat brain: separation and characterization of subunits. *J Biol Chem* 260, 10597-10604.

Miller TC, da Silva D, Miller HA, Kwiecinski H, Mendell JR, Tawil R, McManis P, Griggs RC, Angelini C, Servidei S, Petajan J, Dalakas MC, Ranum LPW, Fu YH, & Ptácek LJ (2004). Correlating phenotype and genotype in the periodic paralyses. *Neurology* 63, 1647-1655.

Moran O, Nizzari M, & Conti F (1999). Myopathic mutations affect differently the inactivation of the two gating modes of sodium channels. *J Bioener Biomem* 31, 591-608.

Nastuk WL & Hodgkin AL (1950). The electrical activity of single muscle fibers. *J Cell Comp Physiol* 35, 39-73.

Nielsen JJ, Mohr M, Klarskov C, Kristensen M, Krustup P, Juel C, & Bangsbo J (2004a). Effects of high-intensity intermittent training on potassium kinetics and performance in human skeletal muscle. *J Physiol (Lond)* 554, 857-870.

Nielsen OB, Örtenblad N, Lamb GD, & Stephenson DG (2004b). Excitability of the t-tubular system in rat skeletal muscle: roles of K^+ and Na^+ gradients and Na^+-K^+ pump activity. *J Physiol (Lond)* 557, 133-146.

Noda M, Shimizu S, Tanabe T, Takai T, Kayano T, Ikeda TS, Takahashi H, nakayama H, Kanaoka Y, Minamino N, Kangawa K, Matsuo H, Raferty M, Hirose T, Inayama S, Hayashida H, Miyata T, & Numa S (1984). Primary structure of electrophorus electricus sodium channel deduced from cDNA sequence. *Nature* 312, 121-127.

Norris Jr. FB (1962). Unstable membrane potential in human myotonic muscle. *Electrocephal Cli Neurophysiol* 14, 197-201.

Okuda S, Kanda F, Nishimoto K, Sasaki R, & Chihara K (2001). Hyperkalemic periodic paralysis and paramyotonia congenita- a novel sodium channel mutation. *Journal of neurology* 554, 857-870.

Patton DE, Isom LL, Catterall WA, & Goldin AL (1994). The adult rat brain beta 1 subunit modifies activation and inactivation gating of multiple sodium channel alpha subunits. *J Biol Chem* 269, 17649-17655.

Patton DE, West JW, & Catterall WA (1992). Amino acid residues required for fast Na^+-channel inactivation: charge neutralizations and deletions in the III-IV linker. *Proc Natl Acad Sci* 89, 10905-10909.

Pearson CM (1964). The periodic paralyses: differential features and pathological observations in permanent myopathic weakness. *Brain* 87, 341-354.

Plassart E, Rime CS, Recan D, Millasseau P, Eymard B, Pelletier J, Thomas C, Chapon F, & Desnuelle C (1994). Mutations in the muscle sodium channel gene (SCN4A) in 13 French families with hyperkalemic periodic paralysis and paramyotonia congenita: phenotype to

genotype correlations and demonstration of the predominance of the two mutations. *European Journal of Human Genetics* 2, 110-124.

Reber BF & Catterall WA (1987). Hydrophobic properties of the beta 1 and beta 2 subunits of the rat brain sodium channel. *J Biol Chem* 262, 11369-11374.

Ricker K, Bohlen R, & Rohkamm R (1983). Different effectiveness of tocainide and hydrochlorothiazide in paramyotonia congenita with hyperkalemic periodic paralysis. *Neurology* 33, 1615-1618.

Ricker K, Camacho LM, Grafe P, Lehmann-Horn F, & Rüdel R (1989). Adynamia episodica hereditaria: what causes the weakness? *Muscle Nerve* 12, 883-891.

Rogart RB, Cribbs LL, uglia LK, & Kephart DD (1989). Molecular cloning of a putative tetrodotoxin resistant rat heart Na^+ channel isoform. *Proc Natl Acad Sci* 86, 8170-8174.

Rojas CV, Wang J, Schwartz LS, Hoffman EP, Powell LS, & Brown RH (1991). A Met-to-Val mutation in the skeletal muscle Na^+ channel a--subunit in hyperkalaemic periodic paralysis. *Nature* 354, 387-389.

Ruff RL (1992). Na current density at and away from endplates on rat fast- and slow twitch skeletal muscle fibers. *Am J Physiol* 262, C229-C234.

Ruff RL (1996). Sodium channel slow inactivation and the distribution of sodium channels on skeletal muscle fibres enable the performance properties of different skeletal muscle fibre types. *Acta Physiol Scand* 156, 159-168.

Ruff RL (1999). Effects of temperature on slow and fast inactivation of rat skeletal muscle Na^+ channels. *Am J Physiol* 277, C937-C947.

Ruff RL, Simoncini L, & Stühmer W (1988). Slow sodium channel inactivation in mammalian muscle: a possible role in regulating excitability. *Muscle Nerve* 11, 502-510.

Sagild U (1963). Hypoglycemia induced by potassium administration during attacks of periodic paralysis. *Acta med scand* 173, 329.

Schaller KL, Krzemien DM, Yarowsky PJ, Krueger BK, & Caldwell JH (1995). A novel, abundant sodium channel expressed in neurons and glia. *Journal of Neuroscience* 15, 3231-3242.

Sejersted OM & Sjogaard G (2000). Dynamics and consequences of potassium shifts in skeletal muscle and heart during exercise. *Physiol Rev* 80, 1411-1481.

Shy GM, Wanke H, Rowley PT, & Engel AG (1961). Studies in familial periodic paralysis. *Exp Neurol* 3, 53-121.

Streeten DHP, Dalakos TG, & Fellerman H (1971). Studies on hyperkalemic peridoic paralysis. Evidence of changes in plasma Na and Cl and induction of paralysis by adrenal glucocorticoids. *J Clin Invest* 50, 142-155.

Struyk AF & Cannon SC (2008). Paradoxical depolarization of Ba^{2+}-treated muscle exposed to low extracellular-K^+: insights into resting potential abnormalities in hypokalemic periodic paralysis. *Muscle Nerve* 37, 326.

Stuhmer W, Conti F, Suzuki H, Wang X, Noda M, Yahagi N, Kubo H, & Numa S (1989). Structural parts involved in activaton and inactivation of the sodium channel. *Nature* 339, 597-603.

Tawil R, McDermott MP, Brown RH, Shapiro BC, Ptácek LJ, McManis P, Marinos DC, Spector SA, Mendell JR, Hahn A, & Griggs RC (2000). Randomized trials of dichlorphenamide in the periodic paralyses. *Annals of neurology* 47, 46-53.

Trimmer JS, Cooperman SS, Tomiko SA, Zhou J, Crean SM, Boyle MB, Kallen RG, Sheng Z, Barchi RL, Sigworth FJ, Goodman RH, Agnew WS, & Mandel G (1989). Primary

structure and functional expression of a mammalian skeletal muscle sodium channel. *Neuron* 3, 33-49.

Van Der Meulen JP, Gilbert GJ, & Kane CA (1961). Familial hyperkalemic periodic paralysis with myotonia. *New England Journal of Medicine* 264, 1-6.

Vilin YY & Ruben PC (2001). Slow inactivation in voltage-gated sodium channels: molecular substrates and contributions to channelopathies. *Journal of Biochemistry and Biophysics* 35, 171-190.

Wallner M, Weigi L, Meera P, & Lotan I (1993). Modulation of the skeletal muscle sodium channel alpha-subunit by the B_1-subunit. *FEBS Lett* 336, 535-539.

Wang J, Rojas CV, & Zhou J (1992). Sequence and genomic structure of the adult human skeletal muscle sodium channel alpha subunit gene on 17q. *Biochem Biophys Res Commun* 182, 794-801.

Wang P & Clausen T (2011). Treatment of attacks in hyperkalemic familial periodic paralysis by inhalation of salbutamol. *Lancet* 1, 221-223.

Weber MA, Nielles-Vallespin SEM, Jurkat-Rott K, Kauczor H, & Lehmann-Horn F (2006). Muscle Na^+ channelopathies: MRI detects intracellular ^{23}Na accumulation during episodic weakness. *Neurology* 67, 1151-1158.

Westerblad H, Lee JA, Lännergren J, & Allen DG (1991). Cellular mechanisms of fatigue in skeletal muscle. *Am J Physiol Cell Physiol* 261, C195-C209.

Yang N, George AL, & Horn R (1996). Molecular basis of charge movement in voltage-gated sodium channels. *Neuron* 16, 113-122.

Yang N, Sen J, Zhou M, Ptácek LJ, Barchi RL, Horn R, & George Jr. AL (1994). Sodium channel mutations in paramyotonia congenita exhibit similar biophysical phenotypes *in vivo.*

Proc Natl Acad Sci 91, 12785-12789.

Yensen C, Matar W, & Renaud JM (2002). The K^+-induced twitch potentiation is not due to longer action potential. *Am J Physiol* 283, C169-C177.

Yu FH & Catterall WA (2003). Overview of the voltage-gated sodium channel family. *Genome Biology* 4, 207-215.

Zhang L, Benson DW, Tristani-Firouzi M, & Ptácek LJ (2005). Electrocardiographic freatures in Andersen-Tawil syndrome patients with KCNJ2 mutations. *Circulation* 111, 2720-2726.

Zhang SJ, Bruton JD, Katz A, & Westerblad H (2006). Limited oxygen diffusion accelerates fatigue development in mouse skeletal muscle. *J Physiol (Lond)* 572, 551-559.

Zhou J & Hoffman EP (1994). Pathophysiology of sodium channelopathies. Studies of sodium channel expression by quantitative multiplex fluorescence polymerase chain reaction. *J Biol Chem* 269, 18563-18571.

Zhou J, Potts JF, Trimmer JS, Agnew WS, & Sigworth FJ (2011). Multiple gating modes and the effect of modulating factors on the ul sodium channel. *Neuron* 7, 775-785.